EXPRESSION, PURIFICATION, AND CHARACTERIZATION OF KYNURENINE FORMAMIDASE FROM *BACILLUS CEREUS.*

by

James M. Bougie

A Thesis
Submitted to the
Graduate Faculty
of
George Mason University
in Partial Fulfillment of
The Requirements for the Degree
of
Master of Science
Chemistry

Committee:

_____	Dr. Timothy Born, Thesis Director
_____	Dr. Barney Bishop, Committee Member
_____	Dr. Robin Couch, Committee Member
_____	Dr. John Schreifels, Department Chairperson
_____	Dr. Timothy L. Born, Associate Dean for Student and Academic Affairs, College of Science
_____	Dr. Vikas Chandhoke, Dean, College of Science

Date: 12/8/2011

Fall Semester 2011
George Mason University
Fairfax, VA

Expression, Purification, and Characterization of Kynurenine Formamidase from *Bacillus cereus.*

A thesis submitted in partial fulfillment of the requirements for the degree of Master of Science at George Mason University

By

James M. Bougie
Bachelor of Science
George Mason University, 2007

Director: Timothy L. Born, Associate Professor
Department of Chemistry and Biochemistry

Fall Semester 2011
George Mason University
Fairfax, VA

DEDICATION

This work is dedicated to my family and friends.

ACKNOWLEDGEMENTS

Dr. Born, for his guidance and support during the course of this project.

Dr. Bishop and Dr. Couch, not only for their expertise but also their willingness to devote their time and energy to refining this manuscript.

Amandeep Kaur and Hashem Mereish, for their time spent assisting me in the purification of NFK.

The Yeh lab at Albert Einstein, for their gift of IDO and their purification procedure.

William Leister, for the use of the instrumentation at NCGC.

Dr. Christopher LeClair, for his expertise regarding NMR spectroscopy and synthetic chemistry.

Tom Daniel, for his willingness to listen to insipid questions about reactions.

Dr. Tim Foley, for our conversation about enzymology.

And finally to the remainder of my friends, family, and co-workers who have given me their support…Thank You.

TABLE OF CONTENTS

Page

LIST OF TABLES VI

LIST OF FIGURES VII

ABSTRACT VIII

INTRODUCTION 1

CLONING, EXPRESSION, AND PURIFICATION OF KFA 13

PURIFICATION OF *N*-FORMYLKYNURENINE (NFK) 21

CHARACTERIZATION OF KFA 25

RESULTS 29

DISCUSSION 53

CONCLUSION 59

REFERENCES 60

LIST OF TABLES

Table Page
KFA EDTA Inhibition Assay Results 48
Comparison of KFA Kinetic Data across Publications.....54

LIST OF FIGURES

Figure Page
Partial Eukaryotic Kynurenine Pathway 3
Saccharomyces cerevisae KFA 9
Saccharomyces cerevisae KFA with Catalytic Triad Highlighted 10
pET100/D-TOPO Vector 15
Binding of 6x-His tagged Protein to Cobalt Metal Affinity Resin 19
BcKynB PCR Reaction Gel with 100 bp Ladder 30
HindIII digestion of pET100 vector with *BcKynB* gene insert and 10,000 bp Ladder 31
SDS-PAGE Gel of KFA Metal Affinity Chromatography Fractions 33
HPLC Trace of IDO Blank Reaction (no enzyme added to reaction vessel) 36
HPLC Trace of a 30 Minute IDO Reaction 37
Purified NFK before Hydrolysis with TFA 38
HPLC Trace of Purified NFK after Incubation with TFA for 60 Minutes 39
HPLC Trace of Overnight Acid Hydrolysis of NFK by TFA 39
LC/MS Trace of Purified NFK 40
NFK NMR Spectrum Peak Identification 41
Full View NMR Spectrum of NFK 42
Magnified View NMR Spectrum of NFK 43
KFA Saturation Curve 44
KFA Solvent Kinetic Isotope Effect Curves 45
KFA pH Dependency Plot (log V) 47
KFA pH Dependence Plot (log V/K) 47
KFA Product Inhibition Assay 49
KFA Product Inhibition Assay (with 200 μM data point removed) 50
Sodium Bisulfite and PMSF Inhibition Assays 52

ABSTRACT

EXPRESSION, PURIFICATION AND CHARACTERIZATION OF KYNURENINE FORMAMIDASE FROM *BACILLUS CEREUS*.

James M. Bougie, M.S.

George Mason University, 2011

Thesis Director: Dr. Timothy L. Born

The kynurenine pathway of tryptophan catabolism in eukaryotes has long been known to be a source of the NAD precursor molecule quinolinic acid as well as immunomodulatory and neuroactive molecules which have been implicated in a wide variety of metabolic disorders and pathologies. Until fairly recently, the kynurenine pathway as it exists in its quinolinate producing role in eukaryotes was thought to be absent in prokaryotes. With the discovery of bacterial genes associated with some of the major enzymes in the pathway in several bacterial species, a "new" source of potential therapeutic targets was revealed.

The complete function of the kynurenine pathway in bacteria is poorly understood due to its fairly recent discovery and resultant lack of mechanistic and structural data regarding its constituent enzymes. In this work, the second enzyme of the kynurenine pathway, kynurenine formamidase (EC 3.5.1.9), was cloned from the genome of *Bacillus cereus* into the pET100/D-TOPO expression vector, expressed in *Escherichia coli*,

purified via metal affinity chromatography, and assayed in order to determine basic kinetic and mechanistic information. While determining the kinetic parameters for the enzyme and comparing them to those found in the literature, the behavior of the enzyme was found to deviate in some cases from the published values. These discrepancies have been noted and will serve as the basis for further study of the enzyme's structure and mechanism.

I. INTRODUCTION

The search for novel antibiotic targets has intensified in recent years due to the emergence of pathogenic bacteria with reduced or eliminated susceptibility to currently prescribed antimicrobials. Methicillin resistant *Staphylococcus aureus* (MRSA), vancomycin-resistant *enterococci*, *Acinetobacter baumannii*, and extremely drug resistant tuberculosis (XDR-TB) strains are a few examples of deadly bacterial species that are highly resistant to our current arsenal of drugs and whose incidence is on the rise [1-4]. While chemical modification of existing antibiotics has been a traditional and productive avenue of antibiotic research, the success of modified compounds is often short lived as bacteria rapidly evolve in response to their administration; often, only a slight modification in the bacterial target renders the new drug ineffective. It is predicted to be more difficult for a bacterial strain to counter a drug which targets a process for which it has no resistance mechanisms in place, thus explaining the driving force toward novel target identification [5].

Ideally, any new drug lead would target cellular machinery unique to prokaryotes in order to limit any toxicity to host cells, and inhibition of the drug target would have either a bactericidal or bacteriostatic effect. While bacteria possess many metabolic pathways that are unique to prokaryotes, and thus are an attractive source for enzyme targets, oftentimes a pathway will be shared with eukaryotes which use “substitutes”, or

isozymes, of the bacterial enzymes in the pathway. The structure of the catalytic domains of these bacterial isozymes often diverges significantly from their eukaryotic counterparts, theoretically allowing for the design of inhibitors that target the bacterial form of the enzyme with high specificity without affecting the eukaryotic isozyme. An example of this would be drugs targeted toward the bacterial ribosome, such as the tetracycline family of antibiotics [6].

One metabolic pathway which is shared between humans and a subset of bacteria is that of tryptophan catabolism, known as the kynurenine pathway. An abridged form of the pathway showing the primary products is illustrated in Figure 1. Tryptophan catabolism has been known for several decades to produce a number of compounds with neuroactive and immunoregulatory functions in humans and other mammals; these compounds are known collectively as the kynurenines. Approximately 99% of ingested tryptophan that is not used in protein synthesis is catabolized via this pathway, making endogenous tryptophan levels a major controller of the availability of important signaling and precursor molecules, including the neuroprotectant kynurenic acid [7, 8] and quinolinate, a known neurotoxin which is also a precursor to nicotinamide. Kynurenic acid and quinolinate exert their effects on the nervous system by acting as antagonists and agonists, respectively, of NMDA receptors [9].

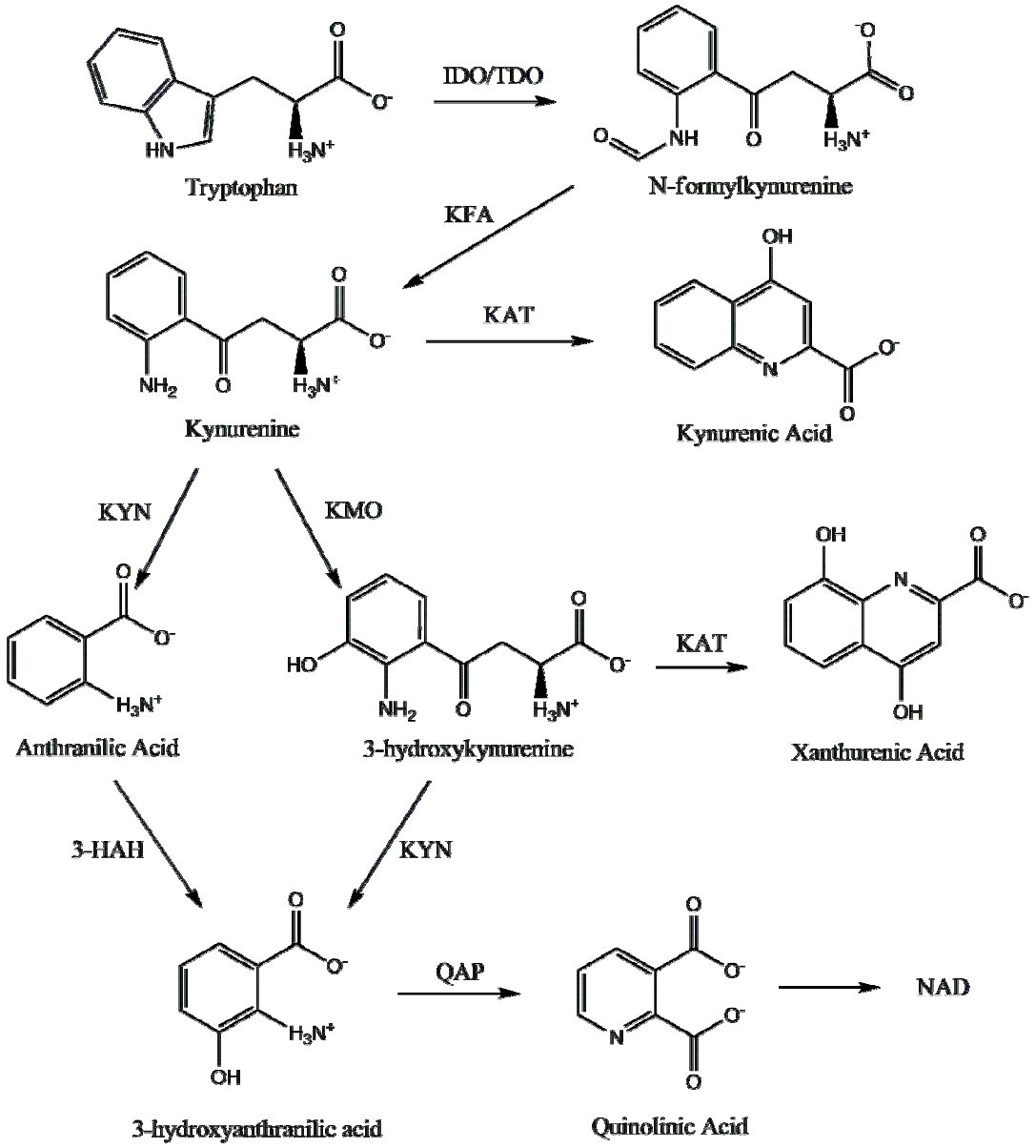

Figure 1 – Partial Eukaryotic Kynurenine Pathway

IDO: Indoleamine 2,3-dixoygenase; TDO: Tryptophan 2,3-dioxygenase; KFA: Kynurenine formamidase; KAT: Kynurenine aminotransferase; KYN: Kynureninase; KMO: Kynurenine Monoxygenase; 3-HAH: 3-hydroxyanthranilic acid hydrolase; QAP: 3-hydroxyanthranilic acid 3,4-dioxygenase

In the first and rate limiting step of the kynurenine pathway, the pyrrole ring of tryptophan is cleaved via addition of molecular oxygen and converted to *N*-formylkynurenine (NFK) by one of two enzymes, indoleamine 2,3-dioxygenase (IDO) or tryptophan 2,3-dioxygenase (TDO). Although these enzymes catalyze identical chemical reactions, they have dissimilar structures and have divergent levels of expression according to cell type, with TDO primarily expressed in hepatic cells and IDO constitutively expressed in the rest of the body [9, 10]. IDO expression is strongly induced by interferon-γ and is known to be involved in a wide variety of cellular processes, including antioxidant activity [9], suppression of the immune system via tryptophan depletion and production of immunoregulatory kynurenines [11], and inflammatory neurological disorders [12]. In addition, elimination of tryptophan by hepatic TDO is a direct regulator of brain serotonin levels and thus may play a prominent role in mood disorders [13].

Once NFK is generated, kynurenine formamidase (KFA) catalyzes a deformylation of the secondary amine, which was formerly part of the indole ring of tryptophan, to form kynurenine. After kynurenine is produced a branching in the pathway occurs (Figure 1). Kynurenine can be hydroxylated to 3-hydroxykynurenine by kynurenine 3-monooxygenase, cleaved by kynureninase (KYN) to form anthranilic acid, or converted to kynurenic acid by kynurenine aminotransferase. Both 3-hydroxykynurenine and anthranilate can be further modified to form 3-hydroxyanthranilic acid by the action of 3-hydroxyanthranilic acid hydrolase or KYN, respectively. Alternatively, 3-hydroxykynurenine can be converted to xanthurenic acid by

kynurenine aminotransferase. Quinolinate is formed by the action of 3-hydroxyanthranilic acid 3,4-dioxygenase and a subsequent non-enzymatically catalyzed ring closure.

The synthesis of quinolinate for use in production of NAD^+ is not limited to eukaryotes. Until recently it was believed that the intact kynurenine pathway was not present in prokaryotes, although individual kynurenine pathway enzymes had previously been isolated from a small number of bacterial species, though without identification of the corresponding bacterial genes. [14]. Instead, these organisms were thought to rely on the catabolism of aspartic acid to form quinolinate via a prokaryotic-specific metabolic pathway [15], while kynurenine pathway enzymes were suspected to be involved with the synthesis of actinomycin in certain *Streptomycin* species [16].

In 2003, this line of thought was overturned when Kurnasov ***et al.*** discovered putative homologs for all kynurenine pathway enzymes in a variety of bacterial species using comparative genome analysis [14].

Gene clusters containing each major kynurenine pathway enzyme, with the exception of KFA, were identified in *Ralstonia metallidurans* and *Cytophaga hutchinsonii*. While a previously unidentified gene encoding for a metal dependent hydrolase in the genome of *R. metallidurans* was eventually found clustered with the genes for TDO and KYN, no such gene could be found in *C. hutchinsonii*. TDO, KFA, KYN, and 3-hydroxyanthranilate-3,4-dioxygenase (HAD) genes were cloned from *R. metallidurans* and transformed into *E. coli* competent cells in order to express their encoded enzymes, while the gene for kynurenine monoxygenase (KMO) was taken from

the genome of *C. hutchinsonii*. Each enzyme was purified via metal affinity chromatography. Kinetic parameters were determined for each enzyme and in some cases brief inhibition studies were performed, such as with KFA. The authors reported that this enzyme was inhibited by EDTA but not PMSF, a known serine hydrolase inhibitor. This supports their previous suggestion that the bacterial KFA enzyme is not homologous to the eukaryotic enzyme.

As mentioned above, two major eukaryotic KFA homologs have been identified and investigated by various groups. First, the murine form of KFA isolated from mouse liver cDNA has been extensively investigated by Casida *et al.*, Pabarcus *et al.*, and Dobrovolsky *et al.* [17-19]. This work [18] determined that the enzyme is an α/β hydrolase based on its amino acid sequence. Kinetic assays performed on the recombinantly expressed wild type enzyme resulted in a specific activity of 42 μmol/min/mg for its natural substrate, NFK [19]. Other kinetic parameters determined included K_m = 0.19 mM and V_{max} = 60 mM/min. Casida's group also generated several mutant forms of KFA using site directed mutagenesis. The targeted residues had been identified as possibly being components of a Ser-His-Asp catalytic triad via computational modeling. Assays performed on the S162A, D247A, and H279A mutants showed that regardless of which residue was mutated, a >99% decrease in activity was observed, thereby substantiating that this enzyme is a serine hydrolase. Also mentioned in this group's work was the previously published promiscuity of the enzyme for amide substrates [20].

In 2007, Wogulis *et al.* determined that a previously identified α/β hydrolase product of the YDR428C gene from *Saccharomyces cerevisae* [21] was a kynurenine formamidase via *in vivo* and *in vitro* biochemical assays, genetic profiling, and crystallography [22]. This KFA homolog possessed 11% identical and 22% similar sequence homology to the murine enzyme. In addition, the catalytic serine residue identified by Pabarcus *et al.* was shown to be in the same position as a serine in the yeast primary structure and was located in the same Gly-Ser-Gly motif, which the authors indicate is prevalent in enzymes possessing an α/β hydrolase structure [23]. A crystal structure of KFA, the first ever generated for a kynurenine formamidase, gave the location of this catalytic serine as being at the bottom of a hydrophobic binding cleft (Fig. 2 and 3). The authors posit that the *N*-formyl moiety of NFK fits into the binding cleft facing the catalytic Ser residue. An oxyanion is then generated from the aldehyde functionality of the compound, which in turn is stabilized by an oxyanion hole laying in close proximity to the binding cleft, enabling the formation of a tetrahedral intermediate.

Assays performed by this group on the isolated yeast KFA with NFK as a substrate resulted in the enzyme having a specificity constant of 8.9×10^5 $s^{-1}M^{-1}$ and a K_m identical to that of the murine enzyme assayed by Casida *et al.*, 0.18 mM, while the k_{cat} calculated from these numbers is approximately 160 s^{-1}. Accurate comparison of the V_{max} values of the two enzymes was rendered impossible due to the unknown concentration of enzyme used in the murine assays; however a rough estimate performed by the authors of the yeast work suggested that the murine enzyme is about 4.7 times slower than the yeast enzyme. *In vivo* studies of yeast KFA showed that knockout

mutants of the gene encoding KFA, *bna7p*, had slower growth in the absence of exogenous nicotinate than both the wild type enzyme and a kynurenine aminotransferase knockout mutant. Although this indicates that KFA is not essential in yeast, it does verify the requirement of KFA for optimal growth

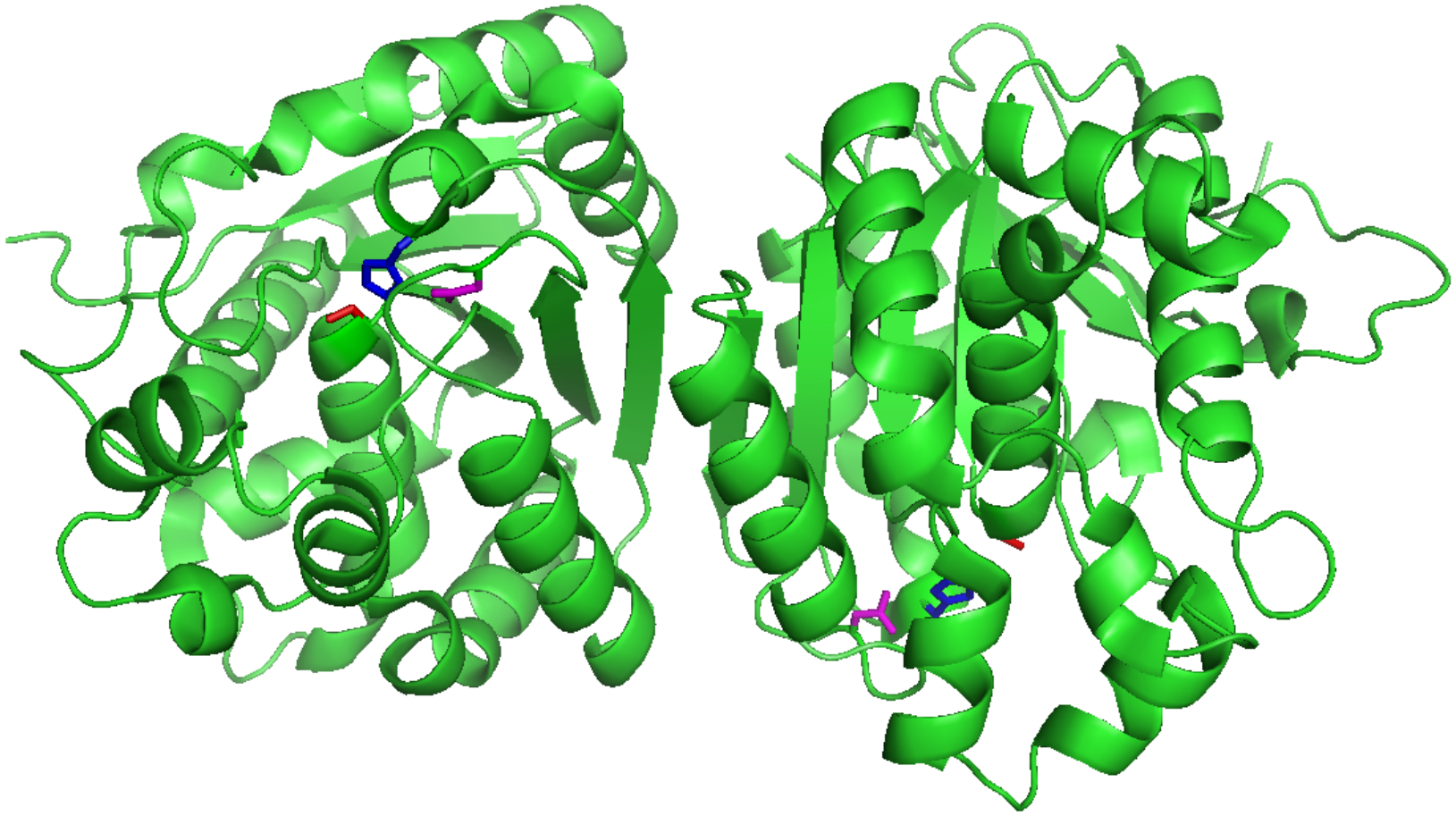

Figure 2 - *Saccharomyces cerevisae* KFA Quaternary Structure [22]. This enzyme exhibits an α/β hydrolase structure [23]

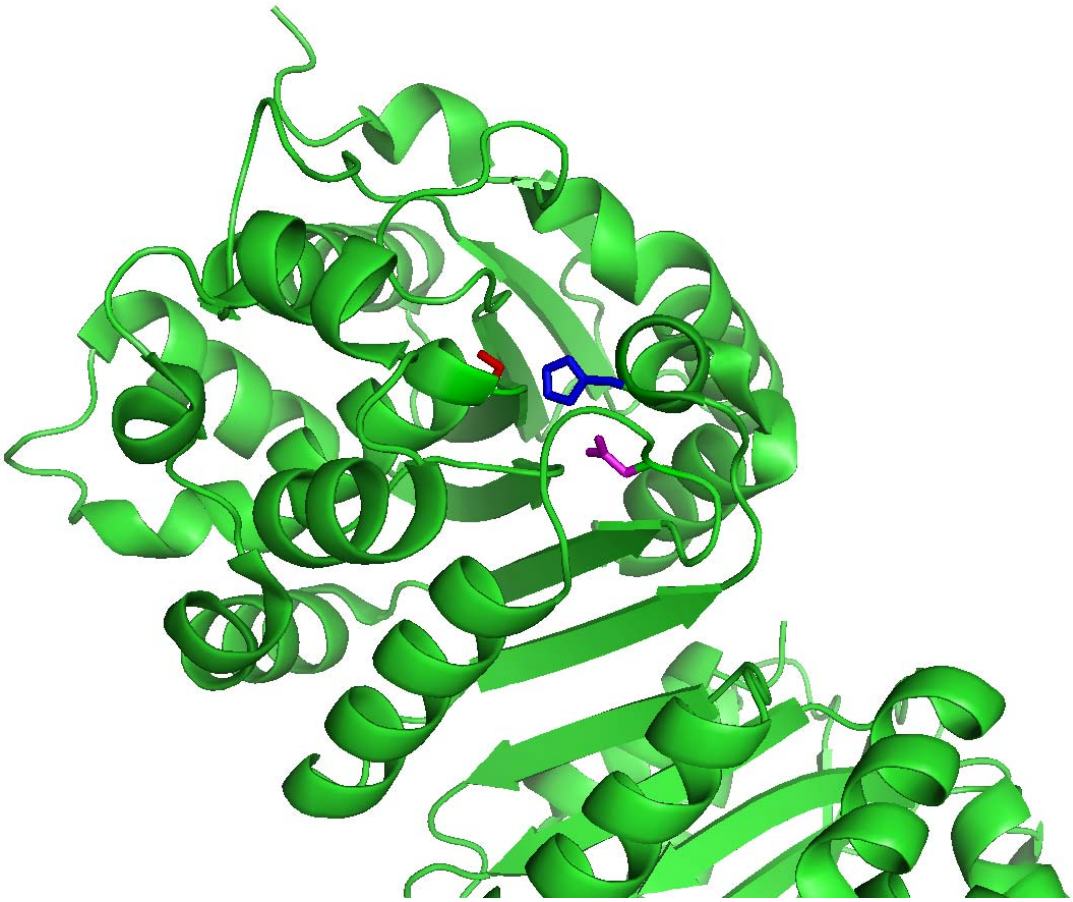

Figure 3 – *Saccharomyces cerevisae* KFA with Catalytic Triad Highlighted [22]

Serine, Histidine, and Aspartic Acid highlighted in red, blue, and purple, respectively.

The focus of this thesis project is on the expression and characterization of kynurenine formamidase (KFA), the second enzyme in the kynurenine pathway, from *Bacillus cereus*. KFA from this particular organism was selected for study due to the fact that our lab has previously worked with unrelated enzymes from this species, thus we have access to a stock of *B. cereus* genomic DNA to use as a source of the KFA gene. To our knowledge only a handful of research groups have investigated KFA and there is still a lack of detailed kinetic information for the enzyme. Most of the information we have is due to the work of Kurnasov *et al.* [24], who cloned, purified, and briefly assayed KFA from *B. cereus, R. metallidurans,* and *Pseudomonas aeruginosa*. This work confirmed the prior discovery that the enzyme is a metal dependent hydrolase with no homologs in either human or yeast genomes.

Basic kinetic assays on bacterial KFA were performed by Kurnasov's group and have provided a starting point from which we have expanded. In addition to determining the specific activity of *B. cereus* KFA to be 5.9 μmol*min^{-1}*mg^{-1}, they performed an EDTA inhibition study [24]. The results of this experiment indicated that complete inhibition of the enzyme could be achieved at an EDTA concentration of 100 μM. This further establishes that KFA is a metal dependent hydrolase. Interestingly, when attempts were made to activate KFA with 20 μM zinc, no effect was seen. The authors explain this as possibly being due to the fact that many hydrolases bind their catalytic metal ions deep within the active site of the enzyme, thus preventing added zinc from having any activating effect [24].

Work performed by Farrow *et al.* in 2007 investigated anthranilate biosynthesis in *P. aeruginosa* by making use of strains of this bacterial species with knockout mutations of the genes encoding for the kynurenine pathway enzymes TDO, KFA, and KYN [25] . Each knockout mutant resulted in a non-existent *Pseudomonas* quinolone signal (PQS) in the case of TDO and KYN knockouts, and a greatly reduced signal was detected for the strain lacking a functional formamidase. This is significant because PQS is an important cell signaling molecule used by the bacterium to regulate virulence factors [26]. In addition, lack of functionality of any of these three enzymes resulted in a reduced ability of *P. aeruginosa* to kill other bacterial species, including *S. aureus*. Expression of TDO and KFA also appeared to be linked to the presence of kynurenine in the cells, as determined by experiments contrasting expression levels in rich and minimal media.

The results of this study suggest that inhibition of the kynurenine pathway via small molecules would be detrimental to bacterial growth, survival, and pathogenesis, specifically by affecting *Pseudomonas* quorum sensing. This information, coupled with the observation that the structure of the enzymes of the bacterial pathway are dissimilar from those in the eukaryotic pathway, indicates that the bacterial kynurenine pathway is potentially a rich source of novel targets for antimicrobial therapies. In addition, the fact that the kynurenine pathway is not present in all bacteria means that any drug developed to disrupt this metabolic pathway would be narrow spectrum, potentially reducing the risk of inadvertent destruction of native bacterial flora.

II. CLONING, EXPRESSION, AND PURIFICATION OF KFA

Cloning

The gene encoding *B. cereus* KFA, *BcKynB*, was PCR amplified using primers complementary to the ends of the gene, which were purchased from Invitrogen. These primers were designed to be used in the pET100/D-TOPO expression system. The sequence of each primer is shown below:

BcKynB-pET100-1: 5'- C ACC *ATG* AAA ACA TCA GAG TGG ATT GAT ATT TCA C-3'

BcKynB-pET100-2: 5'-GC GGA TCC *TTA* TAT TGG TCT AAT AAC GGC TCG AAC-3'

The first primer contains a 4 base pair CACC initial sequence followed by the first codon. The CACC sequence permits directional cloning of the gene into the pET100/D-TOPO vector. The second primer contains a 2 base pair initial sequence followed by a BamHI restriction site. The start and stop codons are highlighted in italics.

The PCR reaction used consisted of the following components: 2 μL of forward primer (200 ng/μL); 2 μL of reverse primer (200 ng/μL); 0.5 μL of *B. cereus* Genomic DNA (200 ng/μL); 22.5 μL of sterile water; 22.5 μL of Finnzymes 2x Master Mix. A

standard set of cycling parameters was used that had been found to be successful with a different *B. cereus* gene [27]. The presence of the PCR product was determined electrophoretically on a 0.8% agarose gel containing ethidium bromide. The gel was run for one hour at 80 volts. Two µL of a 1 kbp DNA ladder was run concurrently with 8 µL of the PCR product in order to evaluate the product's approximate size.

As mentioned previously, the pET100/D-TOPO cloning system from Invitrogen was selected for use as an expression vector (Figure 4). The pET100/D-TOPO vector is an IPTG inducible *lac* operon regulated vector which contains a T7 promoter site, enabling the highly efficient T7 RNA polymerase to be used in gene transcription. Other features of the plasmid include a pre-bound directional topoisomerase (D-TOPO), allowing for quick ligation of the PCR product during cloning; a 6x-Histidine sequence for Histidine tagging of the N-terminus of the enzyme, thus enabling the selective purification of the attached protein using metal affinity chromatography, described later in this section; and the inclusion of an ampicillin resistance marker, allowing for selection of cells that have successfully taken up the plasmid DNA as a result of transformation. This selection is accomplished by plating the transformation reaction on Petri dishes containing growth medium impregnated with ampicillin; all plated cells that do not contain the plasmid, and thus ampicillin resistance genes, will be killed.

Cloning of the PCR product into the pET100/D-TOPO vector was performed according to the protocol supplied by Invitrogen. Three reactions were constructed using three different ratios of insert to vector: 0.5:1, 1:1, and 2:1, with a final vector

concentration of 100 ng/µL in each reaction. In addition, each reaction contained 1 µL of supplied salt solution and distilled deionized water to a final volume of 6 µL.

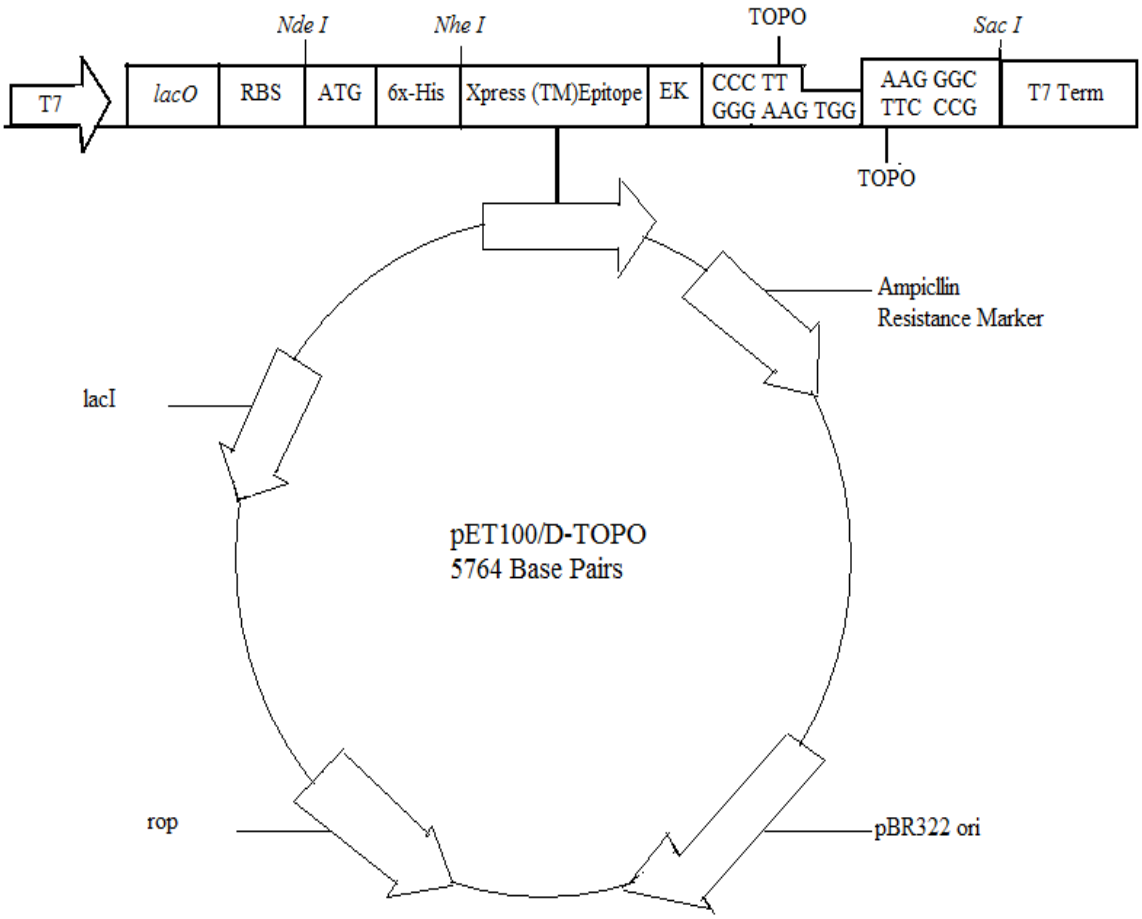

Figure 4 – pET100/D-TOPO Vector (Adapted from figure provided with vector by Invitrogen)

The reactions were mixed gently via pipette and then allowed to incubate at room temperature for 5 minutes. After the ligation reactions were complete, each reaction was transformed into *E. coli* Top10 chemically competent cells purchased from Invitrogen. Three aliquots of cells were thawed on ice, to which 1 µL of a ligation reaction was added. The ligation product/cell mixture was allowed to incubate for 30 minutes on ice, after which the cells were heat shocked at 42°C for 45 seconds. The cells were then immediately placed in ice for 2 minutes, followed by addition of 1 mL of sterile Luria broth to each cell aliquot. The cells were placed in a shaking incubator at 37°C for 1 hour. Once this incubation was complete, the cells were pelleted via centrifugation at 3300×*g* for 2 minutes. The majority of the supernatant was decanted and discarded. The cell pellets were then resuspended in the remaining supernatant by vortexing. The entire resuspended volume of each cell aliquot was spread on LB-agar Petri dishes containing 50 µg/mL ampicillin. The plates were placed in a 37°C incubator and left to grow overnight (~18 hours). All of the ligation reactions produced transformants. Five colonies were isolated from the 1:1 ligation plate and were used to begin five separate 5 mL overnight cultures for use in plasmid purification.

Plasmid DNA was purified from each culture using a Qiagen MiniPrep kit following the supplied protocol. HindIII, a restriction enzyme which cuts once within the pET100 plasmid, was used to linearize the purified DNA prior to analysis via gel electrophoresis. The restriction digest reaction mixture consisted of 1 µL of 10x Buffer M purchased from USB, 1 µL HindIII (also purchased from USB), 4 µL of our purified plasmid, and sterile water to a final volume of 10 µL. Following incubation of the

reaction at 37°C for one hour, each sample was separated on a 1% agarose gel next to a 10 kbp DNA ladder. A sample of this DNA was sent for sequence analysis to Northwoods DNA, Inc., and was shown to contain the intact *BcKynB* gene with no apparent mutations.

Expression

Plasmid DNA containing *BcKynB* was transformed into BL21(DE3) competent *E. coli* cells. This strain of *E. coli* lacks many of the protease enzymes present in other bacterial strains and is thus well suited for protein expression. Cells were plated on LB-agar Petri dishes containing 50 µg/mL ampicillin and incubated overnight at 37°C. Three colonies were selected from this plate and used to inoculate a single 50 mL culture of LB, which was incubated at 37°C overnight. This, in turn, was used to inoculate two 1 L volumes of LB. The OD of these cultures was monitored at 600 nm over a period of ~3 hours. After the OD reached 0.8, protein expression was induced by adding isopropyl-β-D-thiogalactopyranoside (IPTG) to each flask to a final concentration of 1 mM. Expression was allowed to continue for two hours at 37°C, after which the cultures were centrifuged at 2000×*g* for 20 minutes. The supernatant was discarded and the pellets resuspended in a total volume of 50 mL of 25 mM triethanolamine (TEA) buffer, pH 7.8, then frozen at -80°C.

Purification

In order to lyse the cells, lysozyme was added to the resuspended cells to a final concentration of 400 μg/mL and the mixture was incubated with stirring at 4°C for 40 minutes. This was followed by repeated sonication to lyse any remaining intact cells. Each sonication step was conducted on ice at 80% amplitude for one minute, with a total of five sonication steps performed. Afterwards, the lysed cells were centrifuged for 30 minutes at 12,000×g. The supernatant was collected in a beaker and the pellet discarded. The supernatant was incubated with 2 mL of TALON cobalt resin slurry with shaking at 4°C for one hour. The cobalt ions impregnated within the matrix of the resin were effectively chelated by the 6x-histidine tag attached to KFA, thereby selectively binding the enzyme (Fig. 5).

The lysate/resin mixture was poured into an empty chromatography column and fractions were collected via gravity filtration. A filter on the bottom of the column retained the resin but allowed the lysate to flow through; this flow through was saved and labeled as fraction 1. The next four fractions consisted of a wash step using pH 7.8 TEA buffer, a 5 mM imidazole in 25 mM TEA pH 7.8 elution, 200 mM imidazole/TEA elution, and 500 mM imidazole/TEA elution. Each elution fraction had a volume of approximately 8 mL. Samples from each fraction were then analyzed via SDS-PAGE on a PhastGel apparatus. Due to the intensity and thickness of the band resulting from the 200 mM imidazole wash, as well as its relative purity, we proceeded to concentrate this fraction using 10 kDa molecular weight cutoff centrifuge filter columns.

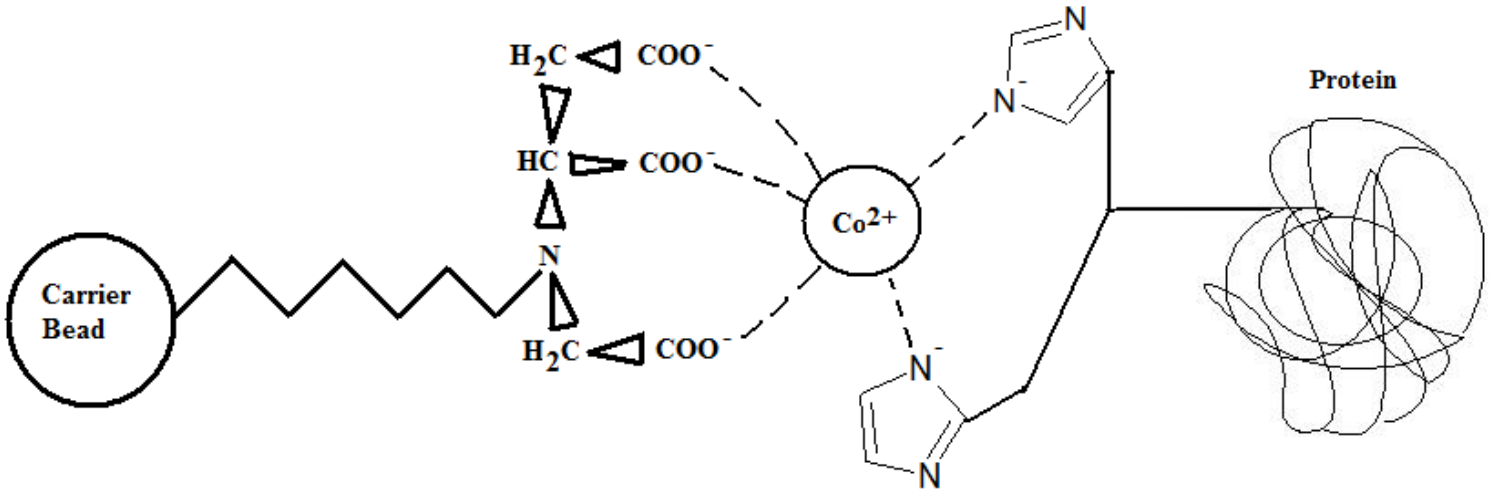

Figure 5 - Binding of 6x-His tagged Protein to Cobalt Metal Affinity Resin (Image adapted from Maryam Goudarzi)

The concentration of the protein was determined spectroscopically using an extinction coefficient of 29,700 $M^{-1}cm^{-1}$, which was acquired using the ExPasy ProtParam online program (http://www.expasy.ch/tools/protparam.html). The protein was aliquoted into a number of microcentrifuge tubes, each with a volume of 500 μL of protein at a concentration of 4 mg/mL. A total of 66 mg of protein was purified, which is typical of the yield using this expression and purification procedure.

After purification, the pelleted protein was resuspended in 25 mM TEA buffer pH 7.8 and frozen under three separate conditions in order to determine optimal conditions for KFA storage. No preservatives were added in the first storage condition. The second storage condition contained 50% glycerol, and the third storage condition contained a final concentration of 1 M ammonium sulfate.

III. PURIFICATION OF *N*-FORMYLKYNURENINE (NFK)

A BL21(DE3)pLysS strain of *E. coli* cells containing an inducible plasmid encoding for human IDO (hIDO) was obtained as a generous gift from the Yeh lab at Albert Einstein College of Medicine. These cells are useful for protein expression for two major reasons. First, they contain the λ-DE3 phage, which enables the expression of T7 RNA polymerase in the host cell. Second, these cells contain the pLysS plasmid. This plasmid encodes for T7 lysozyme, which inhibits the activity of T7 RNA polymerase and thus halts transcription of the T7 promoter regulated hIDO gene prior to induction with IPTG. Induction with IPTG overwhelms the activity of the lysozyme and allows for overexpression of the desired protein. The cells were streaked onto a LB-agar Petri dish containing 50 μg/mL ampicillin and incubated at 37°C for approximately 18 hours. Three colonies from this plate were selected and used to inoculate 50 mL of Luria broth, which was incubated overnight at 37°C with shaking. This culture was used to inoculate two 1 L volumes of Luria broth, which were then incubated at 37°C with shaking. The OD of each culture was monitored at 600 nm for approximately 3 hours. Once each culture had reached an OD of ~0.6, hIDO expression was induced by addition of IPTG to a final concentration of 1 mM. In addition to IPTG, 2 mL of 4 mM heme in 10 mM NaOH was added to each culture, after which the cultures were placed in a shaking incubator and allowed to grow at 25°C overnight.

The next morning, 2 mL of 0.5 M EDTA was added to each culture prior to centrifugation at 2,000×*g* for 20 minutes. The supernatant was discarded and the blood red pellet retained. The cells were resuspended in 50 mL of TEA buffer, pH 7.8, and then lysed using a procedure identical to that described for KFA. The cell lysate was clarified by centrifugation at 12,000×*g* for 30 minutes, after which the supernatant was retained and the pellet discarded. The clarified lysate was incubated with 2 mL of Ni-NTA agarose chelation resin, purchased from GmbH, for 1 hour with shaking. Purification was accomplished using the same gravity filtration methodology described for KFA. Following purification, each fraction was analyzed using a Phastgel apparatus to detect the presence of hIDO. The results of this gel indicated that hIDO was located primarily in the reddish-tinged 200 mM imidazole fraction. No further purification or concentration of this fraction was conducted, and the protein was stored at 4°C.

To produce NFK using the purified hIDO enzyme, a reaction mixture identical to that detailed in a paper by Takikawa *et al.* was constructed [28]. Briefly, a 5 mL solution containing 10 µM methylene blue, 20 mM ascorbic acid, 400 µM tryptophan, water, 50 mM potassium phosphate (pH 6.5), and hIDO was allowed to react for half an hour at room temperature. This reaction was then centrifuged at 4200×*g* for 15-20 minutes to pellet the IDO. The supernatant was drawn out using a syringe and loaded onto an Analogix reverse phase C18 HPLC column which was connected to a Biologic DuoFlow LC system. A buffer consisting of a 9:1 mixture of water to methanol with 10 mM ammonium acetate, pH 6.0, was used to isocratically elute the reaction at a flow rate of 1 mL per minute. The HPLC run was monitored at 321 nm, 365 nm, 220 nm, and 254 nm.

A strong absorption at 321 nm is characteristic solely of NFK out of the components of this particular reaction mixture, while absorption at 365 nm is characteristic of NFK and kynurenine. Organic compounds commonly absorb at wavelengths of 220 and 254 nm. An isolated peak corresponding to NFK was seen after approximately 20 minutes and collected. Methanol was removed from the sample via centrifugal evaporation for approximately 45 minutes. The sample was then frozen in a dry ice/ethanol bath and lyophilized overnight.

After lyophilization was complete, the white powdery NFK was resuspended in 0.5 M phosphate buffer, pH 7.0. A hydrolysis procedure adapted from Takikawa *et al.* [28] was used to determine the yield as well as the extinction coefficient of NFK as follows. A ten microliter aliquot was removed for analysis and the remaining sample was frozen at -20°C. The aliquot was placed in a polypropylene tube, to which was added 2 microliters of 30% TFA. The TFA/NFK solution was incubated at 50°C for ~18 hours to completely hydrolyze the NFK to kynurenine. Afterwards, 10 µL of the sample was diluted to a final volume of 500 µL in a quartz cuvette and an absorbance reading of the sample was taken. Using Beer's Law and a kynurenine extinction coefficient of 4220 $M^{-1}cm^{-1}$ [24], the concentration of NFK present in the cuvette was determined. This concentration was then multiplied by the dilution factor to obtain the original molar concentration of NFK. Beer's law was then used to calculate the extinction coefficient of NFK, which according to our results is 4670 M^{-1} cm^{-1} at 321 nm. Subsequent NFK concentration checks made use of this extinction coefficient, bypassing the hydrolysis procedure.

LC/MS analysis of purified NFK was performed using an Agilent 1200 system. Separation was achieved using a Phenomenex Luna 75 x 3.0 mm, 3 micron reverse phase column. Two mobile phases, A and B, were used in the analysis gradient. Mobile phase A consisted of analytical grade water with 0.05% TFA added, and mobile phase B consisted of analytical grade acetonitrile with 0.025% TFA added. An injection of 3 μL of NFK solution was eluted using a gradient of 4 to 100% acetonitrile over 4 minutes.

The same batch of purified NFK was then dried via lyophilization and resolubilized in deuterium for NMR analysis on a Varian 400 MHz instrument.

IV. CHARACTERIZATION OF KFA

KFA spectrophotometric assays were conducted using a Uvikon 933 double beam UV/VIS spectrophotometer. Our basic assay composition is adapted from that used by Kurnasov *et al.* in their work [24]. Each reaction contained 20 μM zinc chloride, 10 μg KFA, 100 mM sodium or potassium phosphate pH 7.5 buffer, and de-ionized distilled water (ddH_2O) to a final volume of 500 μL, unless otherwise noted.

KFA Saturation Curve

The dependence of KFA activity on the concentration of NFK was determined by assaying the enzyme at NFK concentrations of 10, 15, 25, 50, 75, 100, 125, 150, 175, and 200 μM. Each concentration was assayed in duplicate. The formation of the reaction product, kynurenine, was monitored at 365 nm for two minutes. Slopes were then calculated for each reaction's initial velocity. Slopes were converted to velocities and the data was fit to the Michaelis-Menten equation (Eq.1) using SigmaPlot version 10:

$$\nu = V_{max}[S]/K_m + [S] \qquad \text{(Eq.1)}$$

Solvent Kinetic Isotope Effects

Solvent kinetic isotope effects were determined by use of enzymatic assays containing 80% deuterated water (D_2O). A saturation curve was constructed using reaction mixtures with compositions identical to that described above and NFK concentrations of 10, 25, 50, 100, 150, and 200 μM. In addition, a set of reactions with the same NFK concentrations were constructed in 80% D_2O by using 400 μL of D_2O in place of ddH_2O. The slope obtained from each reaction was converted to a velocity and kinetic parameters were determined by fitting the velocities to the Michaelis-Menten equation (Eq.1).

Effect of pH on KFA Kinetics

Reaction mixtures utilizing various pH buffers were used to determine the effect of the protonation state of the enzyme on its ability to catalyze the NFK/KYN reaction. pH values were varied between 5.5 and 9.5 to determine the optimum pH for KFA activity as well as the pK_a values of important ionizations. Saturation curves were constructed using NFK concentrations of 10, 25, 50, 100, 150, and 200 μM. Two buffer solutions were used to complete the pH range. For pH 5.5 to 8.5, 50 mM sodium or potassium phosphate was used. For pH 9.0 and 9.5, 50 mM *N*-Tris(hydroxymethyl)methyl-3-aminopropanesulfonic acid (TAPS) was used. No buffer effect on the rate of KFA catalysis was observed when separate reactions run at pH 8.0 using TAPS and phosphate buffers were compared.

The kinetic values V_{max} and V_{max}/K_M were determined and the data were fit to Eq. 2 using SigmaPlot:

$$\log V = \log[C/(1 + H/K_a)] \qquad \text{(Eq. 2)}$$

where V is the maximal velocity (or V_{max}/K_M), C is the pH-independent plateau value, H is the hydrogen ion concentration, and K_a is the ionization constant for the acidic group.

Inhibition of KFA by addition of EDTA

KFA reaction mixtures containing variable amounts of EDTA were assayed to determine what effect addition of this chelating agent exerted on KFA catalysis. Reaction mixtures containing KFA, water, sodium phosphate, and zinc were made in identical concentrations to those described for the construction of the saturation curve. EDTA was added to each mixture in concentrations of 0, 25, 50, 100, 150, 200, and 400 μM. The reactions were allowed to incubate for approximately 10 minutes, after which the reaction was initialized via addition of NFK to a final concentration of 100 μM. Reaction rates were monitored via the same method described above.

Inhibition of KFA by addition of Kynurenine

KFA reaction mixtures containing variable amounts of kynurenine were assayed to determine whether the enzyme is inhibited by its reaction product as well as the type of inhibition displayed, if any. Reaction mixtures containing 100 μM NFK and zinc, sodium

phosphate, and water in concentrations identical to those described for the initial saturation curve reactions were made. Kynurenine was added incrementally at final concentrations of 0, 25, 100, 150, 200, and 400 μM. The reactions were initiated by addition of enzyme and rates were monitored using the same method described above.

Inhibition of KFA by addition of phenylmethylsulfonyl fluoride (PMSF)

KFA reaction mixtures containing fixed concentrations of PMSF were assayed to determine whether or not *B. cereus* KFA can be inhibited by a potent known inhibitor of the eukaryotic KFA enzyme. Reaction mixtures containing KFA, water, sodium phosphate, and zinc were made in identical concentrations to those described for the construction of the saturation curve. PMSF was added to each mixture in concentrations of 0, 25, 50, 100, 150, 200, and 400 μM. Reactions were initialized via addition of KFA. Reaction rates were monitored via the same method described above.

Inhibition of KFA by addition of sodium bisulfite

KFA reaction mixtures containing fixed concentrations of sodium bisulfite (NaBis) were assayed to determine whether or not *B. cereus* KFA can be inhibited by a known inhibitor of the *S. parvulus* KFA enzyme. Reaction mixtures containing KFA, water, sodium phosphate, and zinc were made in identical concentrations to those described for the construction of the saturation curve. NaBis was added to each mixture in concentrations of 0, 25, 50, 100, 150, 200, and 400 μM. Reactions were initialized via addition of KFA. Reaction rates were monitored via the same method described above.

V. RESULTS

Cloning, Expression, and Purification of KFA

The gene encoding for *B. cereus* KFA, *BcKynB*, was PCR amplified and analyzed using gel electrophoresis. *BcKynB* is 623 bp in length, therefore the band that was visualized at ~650 bp indicated that the PCR reaction successfully amplified the gene of interest (Figure 6). Note that this picture was taken of a gel run of a *BcKynB* PCR product amplified using Gateway cloning system primers; however our pET100 PCR reactions produce a gel identical to that pictured.

After the presence and size of the PCR product was validated it was cloned into the pET100/D-TOPO bacterial expression vector purchased from Invitrogen. Three different ligation reactions containing three different ratios of insert to vector were constructed, as recommended by the supplied manual. A volume of 1 μL from each ligation reaction was used to transform Top10 *E. coli* cells. A number of overnight cultures were started from the 1:1 ligation plate and were allowed to grow for an ~18 hour period. Plasmid DNA was purified from these cell cultures using a Qiagen MiniPrep kit, linearized by incubation with HindIII for 1 hour, and analyzed via agarose gel electrophoresis along with a TrackIt 1 kb DNA ladder (Figure 7). HindIII cuts the pET100 vector once at 709/713 bp, theoretically resulting in a single band at 6387 bp, the length

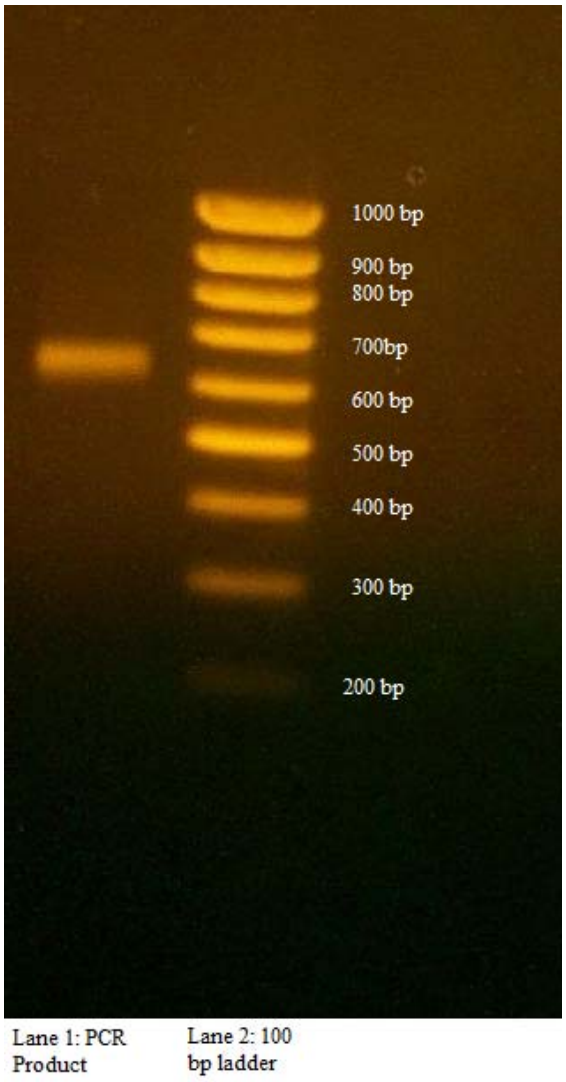

Figure 6 - *BcKynB* PCR Reaction Gel with 100 bp Ladder

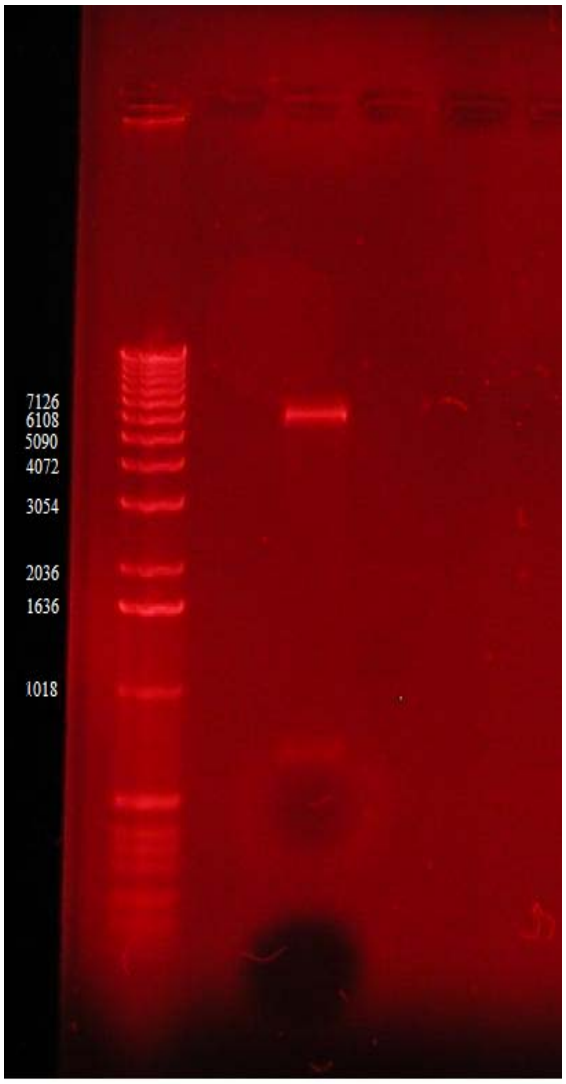

Figure 7 - HindIII digestion of pET100 vector with *BcKynB* gene insert and 10,000 bp Ladder

of the pET100 plasmid with the *BcKynB* gene inserted, compared to the original uncut plasmid size of 5764 bp. This single band is clearly visible and is located between the 6000 and 7000 bp ladder bands, as expected.

The purified plasmid DNA was transformed into BL21 (DE3) strain *E. coli* cells for protein production. Cultures of the transformants were induced with 1 mM IPTG and incubated at 37°C for two hours, after which the cells were pelleted, resuspended, and lysed as described. The lysate was incubated with TALON cobalt metal affinity resin for 1 hour at 4°C with shaking. The lysate and resin mixture was decanted into a chromatography column which retained the resin while allowing the lysate to flow through and be collected. Separately, a total of four ~8 mL wash steps were performed after the flow through was collected, including a TEA buffer wash, 5 mM imidazole in TEA, 200 mM imidazole in TEA, and 500 mM imidazole in TEA. Each fraction was analyzed via SDS-PAGE in a PhastGel apparatus, resulting in the gel shown in Figure 8.

Fractions 3, 4, and 5 were determined to have a band of the correct size (~23 kDa) via comparison with a molecular weight ladder run simultaneously with the collected fractions, seen in the first lane. Fraction 4 was concentrated using 10 kDa cutoff centrifugal filter devices and divided into 4 mg/mL aliquots, each containing either 1 M ammonium sulfate, 50% glycerol, or no additional compound in order to determine optimal storage conditions. Approximately one month after freezing at -20°C, enzyme activity was evaluated and compared to that of the freshly purified enzyme. The stocks with no added preservatives were significantly less active, and interestingly the glycerol

stocks were almost completely inactive. The enzyme frozen with 1 M ammonium sulfate was fully active by comparison and reactions were conducted with these aliquots.

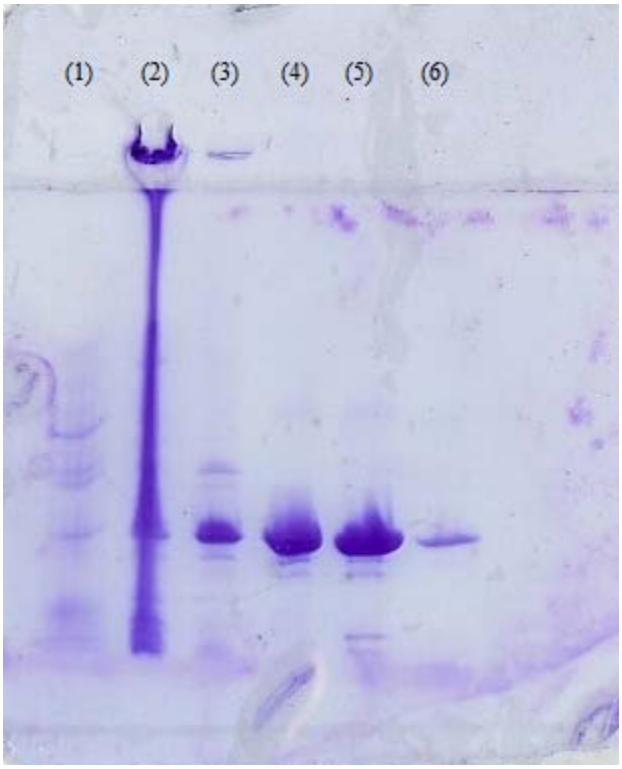

Figure 8 – SDS-PAGE Gel of KFA Metal Affinity Chromatography Fractions. From left to right: (1) 10 kDa molecular weight marker; (2) Crude lysate; (3) TEA buffer wash; (4) 5 mM imidazole wash; (5) 200 mM imidazole wash; (6) 500 mM imidazole wash

Purification of NFK

The substrate for KFA, NFK, is not cheaply purchased, which forced us to find a way to produce the compound. Initially, we intended to chemically synthesize NFK using a slight variation of the single step reaction method of Dalgliesh *et al.* [29], which uses commercially available kynurenine as a starting material. In this reaction, 100 µL of

formic acid and 50 μL of acetic anhydride were combined and allowed to stand for 30 minutes. Next, 103 mg of kynurenine was added to the mixture and the solid immediately went into solution, which became a very dark brown. The reaction was allowed to proceed for 2 hours, after which the entire volume of the reaction was gradually poured with stirring into 50 volume equivalents of anhydrous ether at 0°C. Crystallization proceeded for 2 hours, during which time the previously brown, glassy solid became lighter in tone and more granulated in appearance. Unfortunately, this product was determined by UV spectroscopy to be kynurenine rather than the expected NFK.

Repeated attempts at this synthesis and slightly altered versions continued to result in failure for unknown reasons, necessitating a re-evaluation of how to best produce the compound. A literature search revealed that the Yeh lab at Albert Einstein College of Medicine had successfully cloned the gene for human indoleamine 2,3-dioxygenase (hIDO) into an *E. coli* expression vector. From this group, we obtained *E. coli* pLysS strain cells expressing hIDO as well as a detailed procedure for expressing and purifying hIDO, for which we are extremely grateful. Once IDO was purified, an enzymatic reaction adapted from that used by Takikawa *et al.* in their work with IDO was used to produce NFK. This reaction consists of tryptophan, methylene blue, ascorbate, pH 6.5 phosphate buffer, water, and IDO. Tryptophan serves as the enzyme's substrate, while methylene blue and ascorbate act as an electron carrier and donor, respectively [10].

A "blank" reaction lacking IDO was loaded onto a C18 reverse phase HPLC column and isocratically separated with a 9:1 mixture of water to methanol containing 10

mM ammonium acetate at a flow rate of 1 mL per minute, which is identical to that published by Takikawa's group. Four primary wavelengths were monitored: 321 nm, 365 nm, 220 nm, and 254 nm. Absorbances at 321 nm and 365 nm are characteristic of NFK and kynurenine, respectively, while 220 nm and 254 nm are common absorbance wavelengths of organic compounds corresponding to carbonyl groups and ring system conjugation, respectively. The resulting chromatogram is shown in Figure 9.

Previous literature HPLC analysis of the individual components of the hIDO reaction mixture enabled the identification of each peak seen above [28]. The peak occurring at approximately 5 minutes corresponds to methylene blue, while the peak at ~34 minutes is tryptophan. After the blank was run, a reaction containing hIDO was incubated for 30 minutes at room temperature, centrifuged at 4200×*g* for 20 minutes to pellet the enzyme, and then loaded onto the HPLC column. The elution protocol and wavelengths monitored were identical to that of the blank reaction. The resulting chromatogram is shown in Figure 10. The new peak eluting at ~21 minutes corresponds to NFK, as it is the only reaction component absorbing appreciably at 321 nm, a wavelength at which NFK has been previously documented to absorb [14, 24].

This initial reaction was scaled up five-fold and used to produce significant quantities of NFK. Because divergent extinction coefficients for NFK exist in the literature, a hydrolysis procedure adopted from Takikawa *et al.* was used to hydrolyze NFK to kynurenine in order to determine an extinction coefficient under the specific conditions in our laboratory. Two separate aliquots consisting of 1 μL of concentrated TFA and 9 μL of NFK were made and placed in thin walled thermally conductive

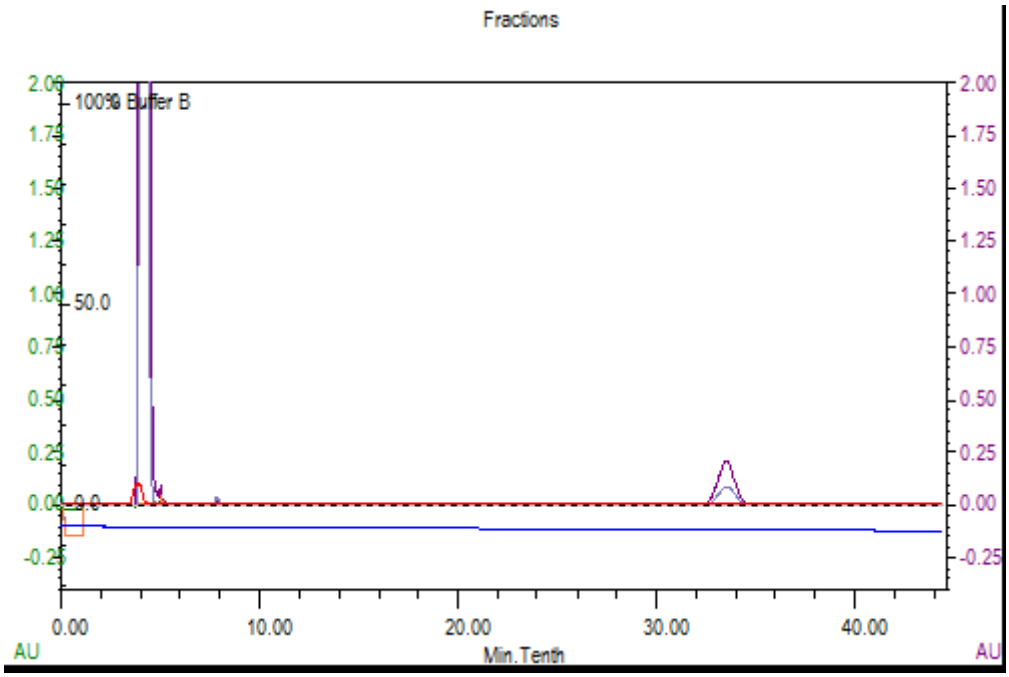

Figure 9 – HPLC Trace of IDO Blank Reaction (no enzyme added to reaction vessel)

Note: The key wavelengths in this chromatogram and the chromatograms depicted in Figures 10-13 are 321nm (colored orange) and 365 nm (colored purple). Blue and Green correspond to 254 and 220 nm, respectively.

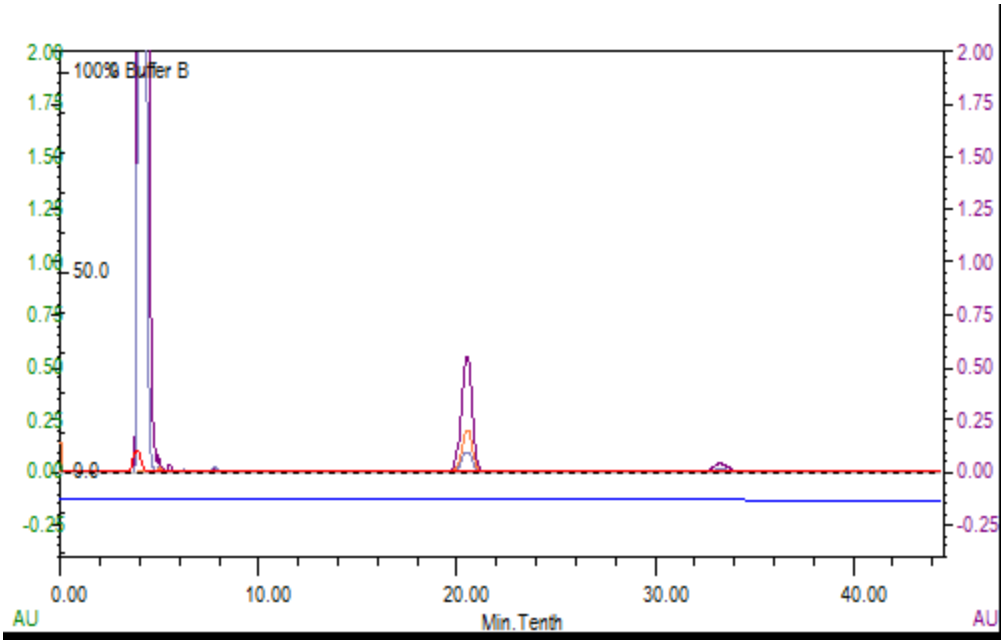

Figure 10 – HPLC Trace of a 30 Minute IDO Reaction

polypropylene tubes. Both tubes were incubated at 50°C on a programmable heat block. One aliquot was allowed to react for 1 hour, while the other aliquot was incubated overnight. After each reaction was complete, the entire mixture was analyzed via HPLC using the same instrumentation and methodology described above. The resulting chromatograms are shown in Figures 12 and 13 along with a reference standard of purified NFK in Figure 11. These chromatograms show that hydrolysis of NFK was incomplete after the one hour incubation time, but that the overnight incubation resulted in complete conversion of NFK to kynurenine. The overnight incubation was repeated and the concentration of kynurenine was determined using Beer's law. This concentration was then used to back-calculate the original concentration of NFK. From these

calculations we determined the extinction coefficient of NFK to be 4670 M^{-1} cm^{-1} at 321 nm.

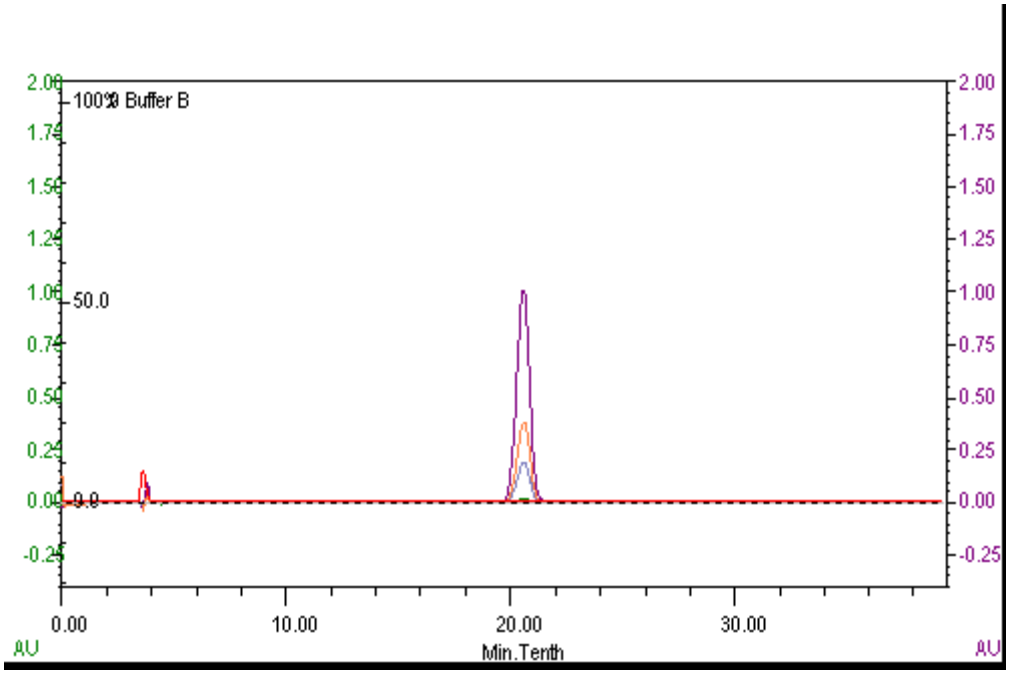

Figure 11 – Purified NFK before Hydrolysis with TFA

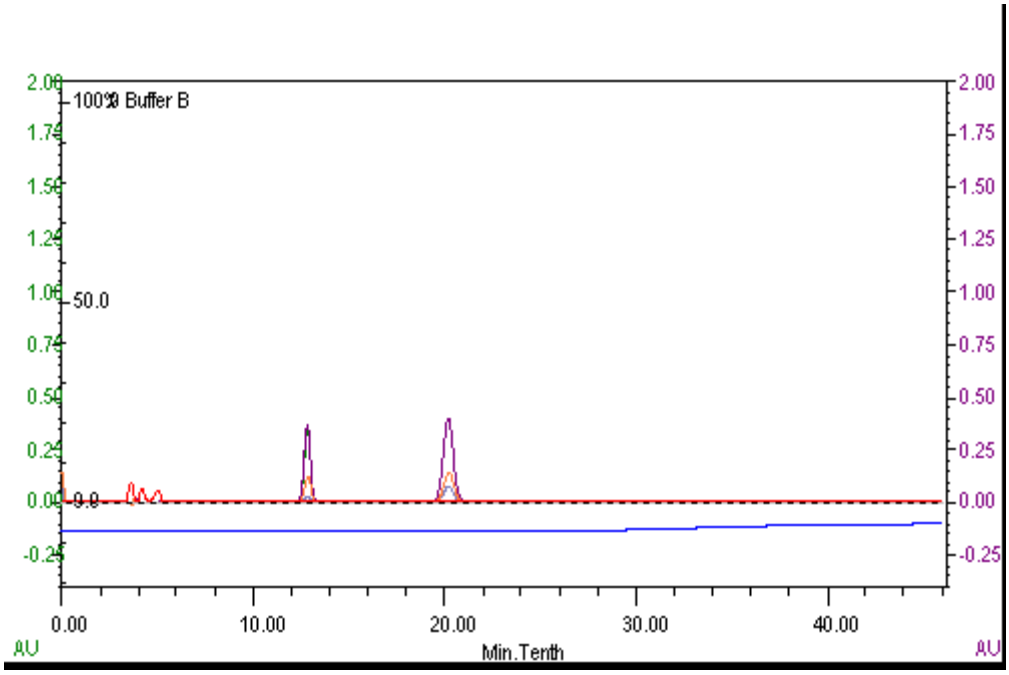

Figure 12 – HPLC Trace of Purified NFK after Incubation with TFA for 60 Minutes

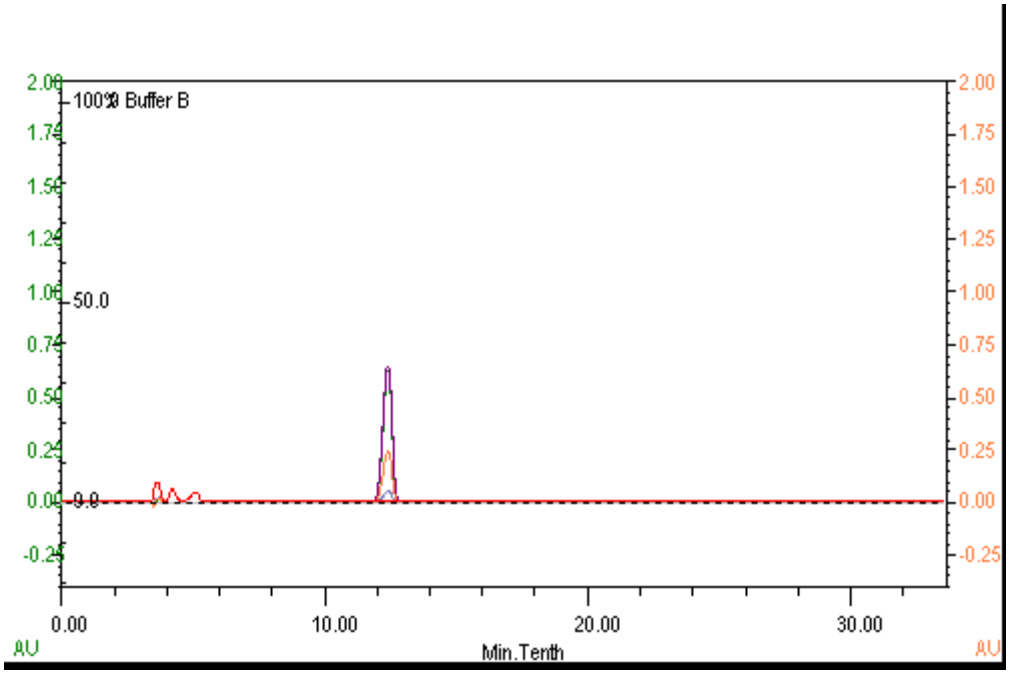

Figure 13 – HPLC Trace of Overnight Acid Hydrolysis of Purified NFK by TFA

LC/MS analysis of purified NFK was performed using an Agilent 1200 LC and Agilent 6130 single quadrupole MS instrument. The resulting LC/MS trace is shown in Figure 14.

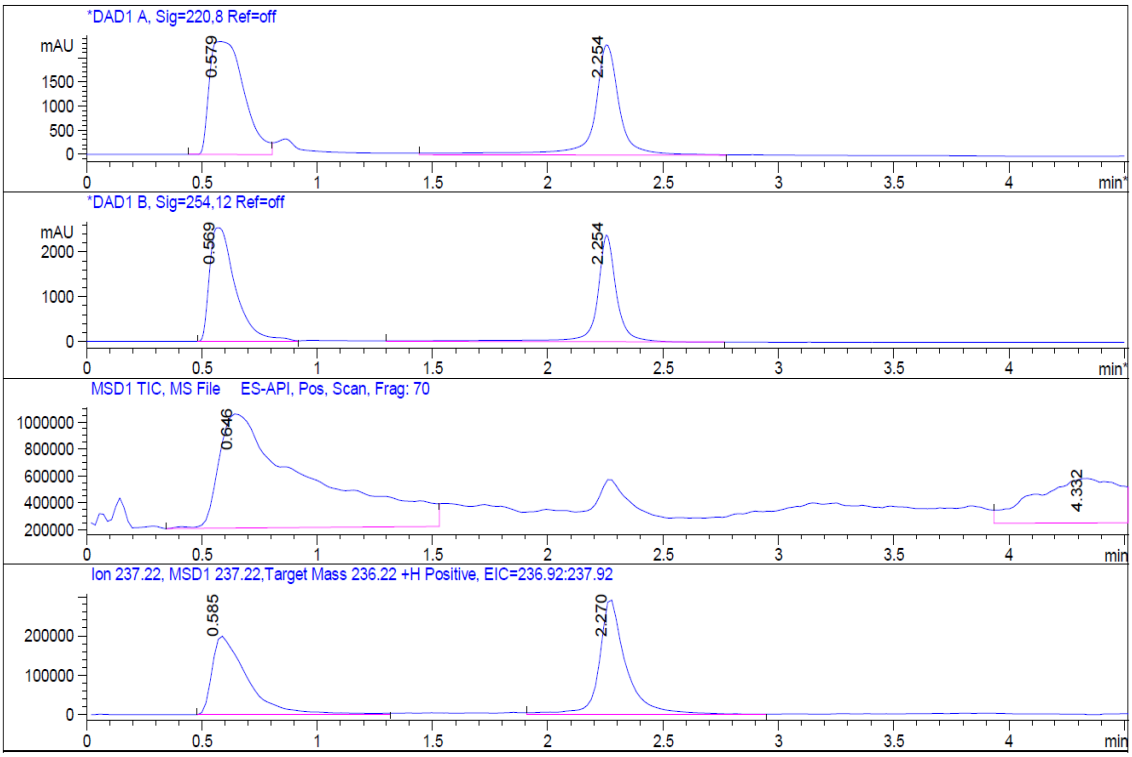

Figure 14 – LC/MS Trace of Purified NFK

Note that the void peak eluting at 0.579 minutes contains the NFK+H ion in addition to the compound peak eluting at 2.254. This phenomenon is compound rather than strictly concentration specific and is likely due to the column being overloaded because the limited surface area of the stationary phase was not able to interact with the

entirety of the NFK molecules. The sample above was diluted tenfold with no success in eliminating this void peak.

Purified NFK was further analyzed using a Varian 400 MHz 1H NMR. The spectrum obtained is of ~2 mg of NFK dissolved in D_2O (Table 1). Each peak was identified as shown in Figure 15:

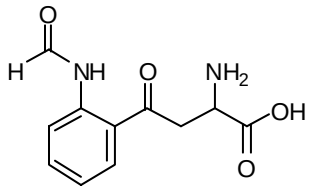

***N*-formylkynurenine** ^{1}H NMR (400 MHz, D_2O)

δ 8.35 (s, 1H, CHO),
8.15 (d, 1H, *J* = 8.4 Hz, PhH),
7.99 (d, 1H, *J* = 8.0 Hz, PhH),
7.66 (t, 1H, *J* = 7.6 Hz, PhH),
7.35 (t, 1H, *J* = 7.6 Hz, PhH),
4.16 (t, 1H, *J* = 5.3 Hz),
3.75-3.78 (m, 2H),
No NH or OH signals.

Figure 15 – NFK NMR Spectrum Peak Identification

The full spectrum obtained from the experiment as well as an enhanced view of the significant portion of the spectrum is shown in Figure 16 and 17, respectively.

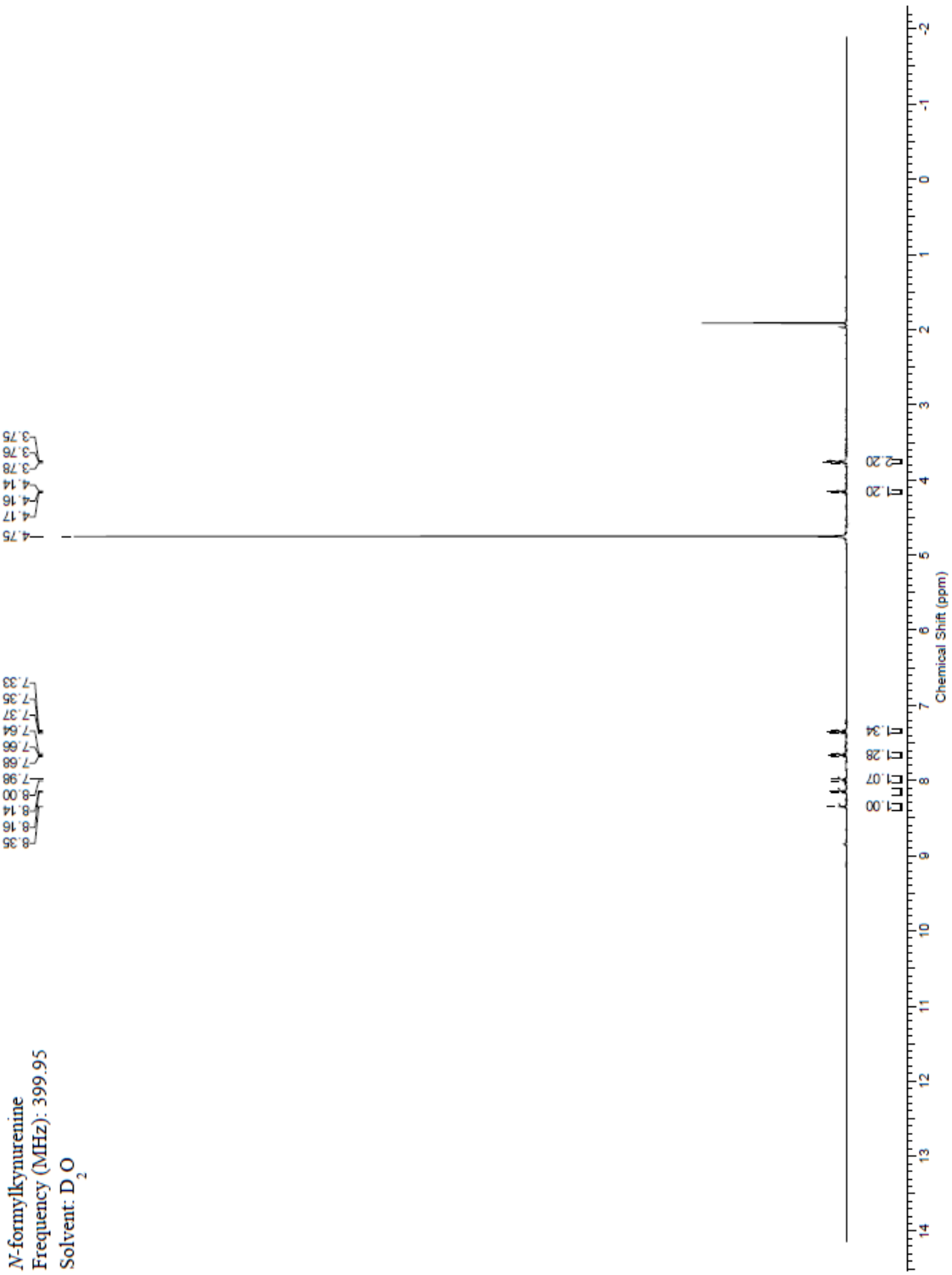

Figure 16 – Full View NMR Spectrum of NFK

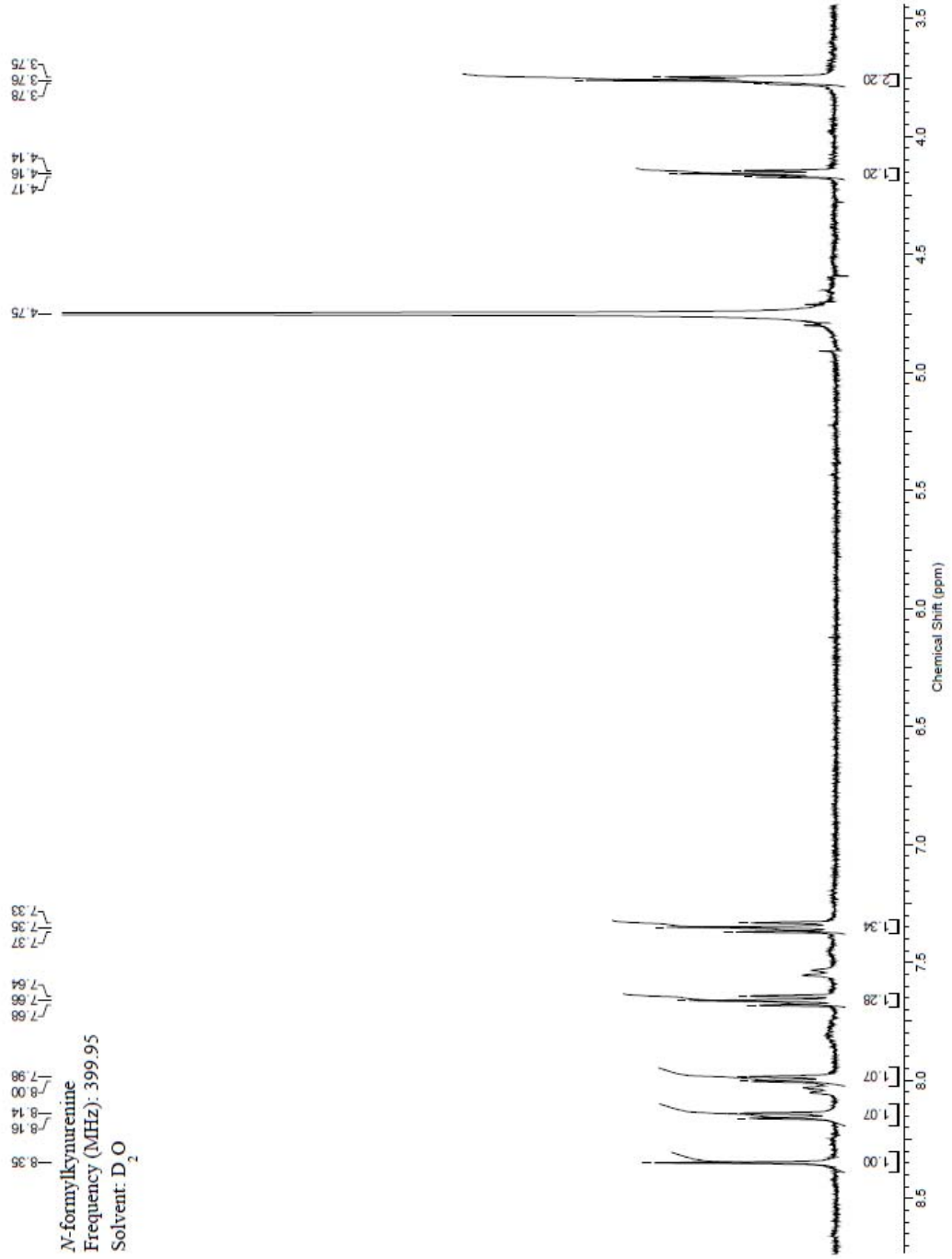

Figure 17 – Magnified NMR Spectrum of NFK

Characterization of KFA

KFA Saturation Curve

To begin the characterization of KFA, a saturation curve was constructed using variable concentrations of NFK. Slopes for each substrate concentration were converted to velocities and these velocities were fit to a hyperbola. The resulting curve is shown in Figure 18.

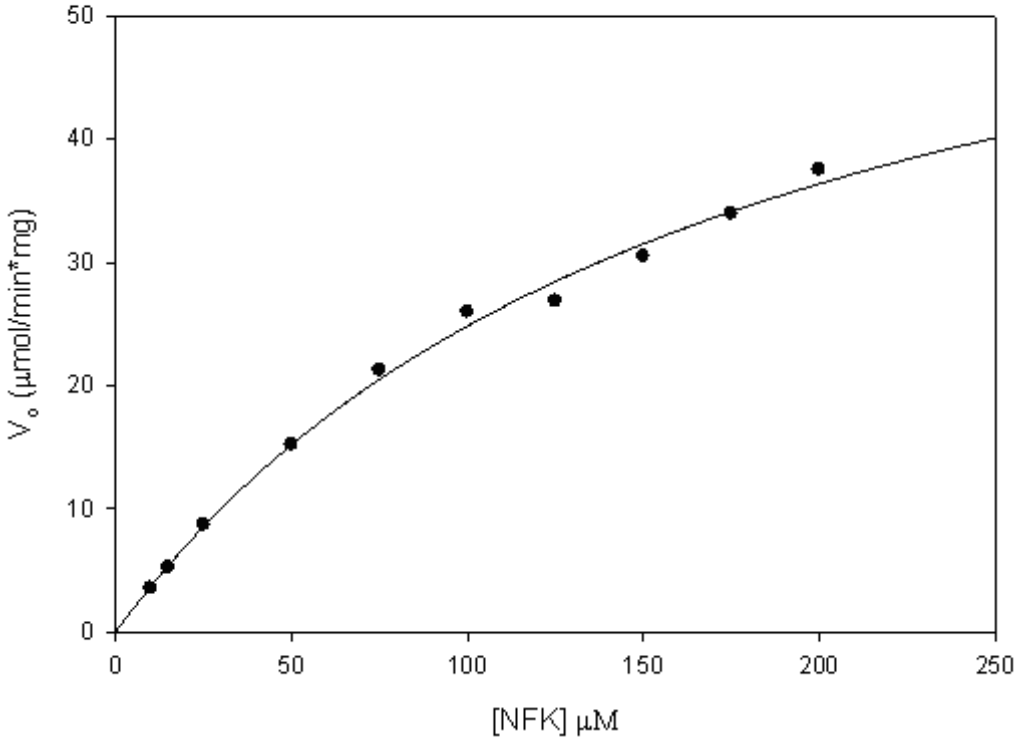

Figure 18 – KFA Saturation Curve

As can be seen from Figure 17, KFA follows Michaelis-Menten kinetics, so eq. 1 was used to determine kinetic values for the enzyme. The values for V_{max} and K_m were determined to be 68 ± 5 μmol/min*mg and 170 ± 20 μM, respectively.

Solvent Kinetic Isotope Effects

Solvent kinetic isotope effects were determined by comparing the rate of reaction of KFA in 100% H_2O and 80% D_2O. Slopes obtained from monitoring the reactions at 365 nm were converted to velocities and fit to Eq. 1. The resulting plot is shown in Figure 19, where it is apparent that the reaction proceeds faster in H_2O than in D_2O.

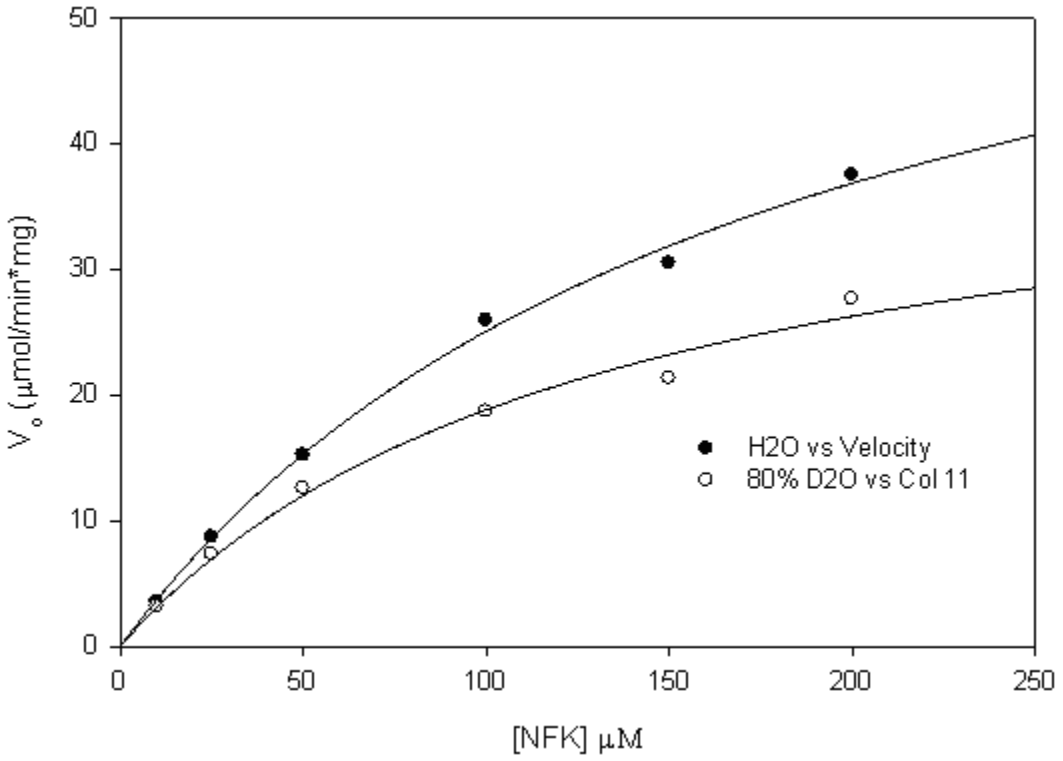

Figure 19 – KFA Solvent Kinetic Isotope Effect Curves

pH Data

The pH-dependence of the KFA reaction was determined by varying the pH of the reaction mixture from 5.5 to 9.5. Slopes obtained from monitoring the formation of kynurenine at 365 nm were converted to velocities for a total of six substrate concentrations. The log of each velocity was plotted against pH and is represented in Figure 20. In addition, a separate plot was created where each velocity was divided by the respective K_m value. The logarithm of each V/K value was taken and then plotted versus pH. This plot is depicted in Figure 21. Both plots show that the enzyme activity decreases as the pH is lowered, indicating the presence of a single ionizable group that must be deprotonated for maximal activity. Fitting of the data to equation 3 yielded pK_a values of 6.3 for log V and 6.7 for log V/K.

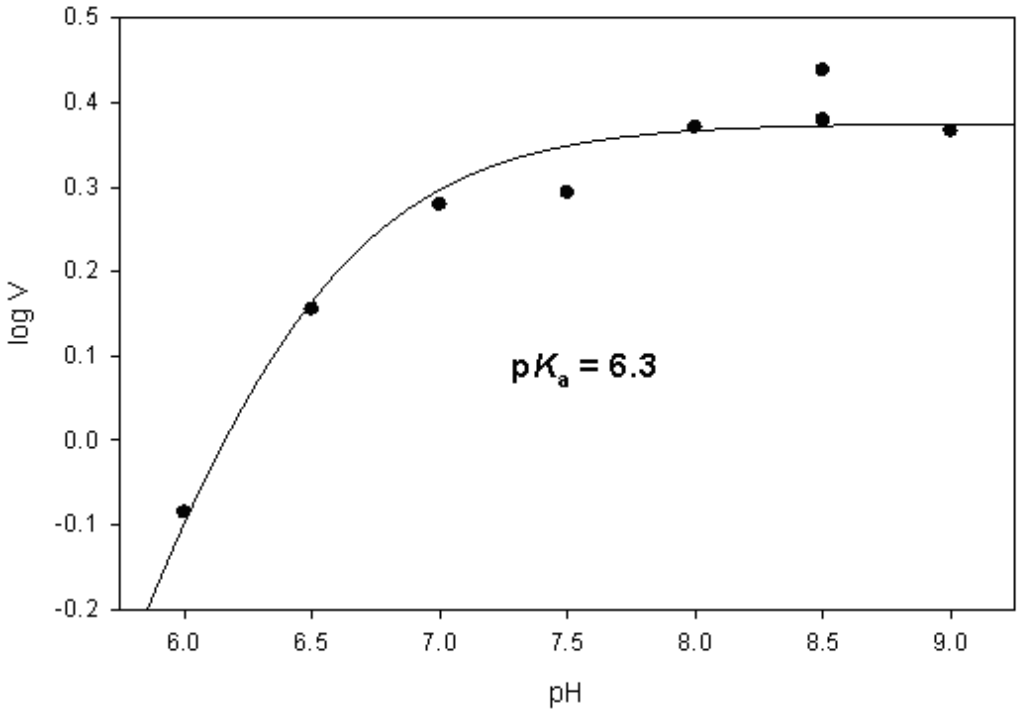

Figure 20 – KFA pH Dependency Plot (log V)

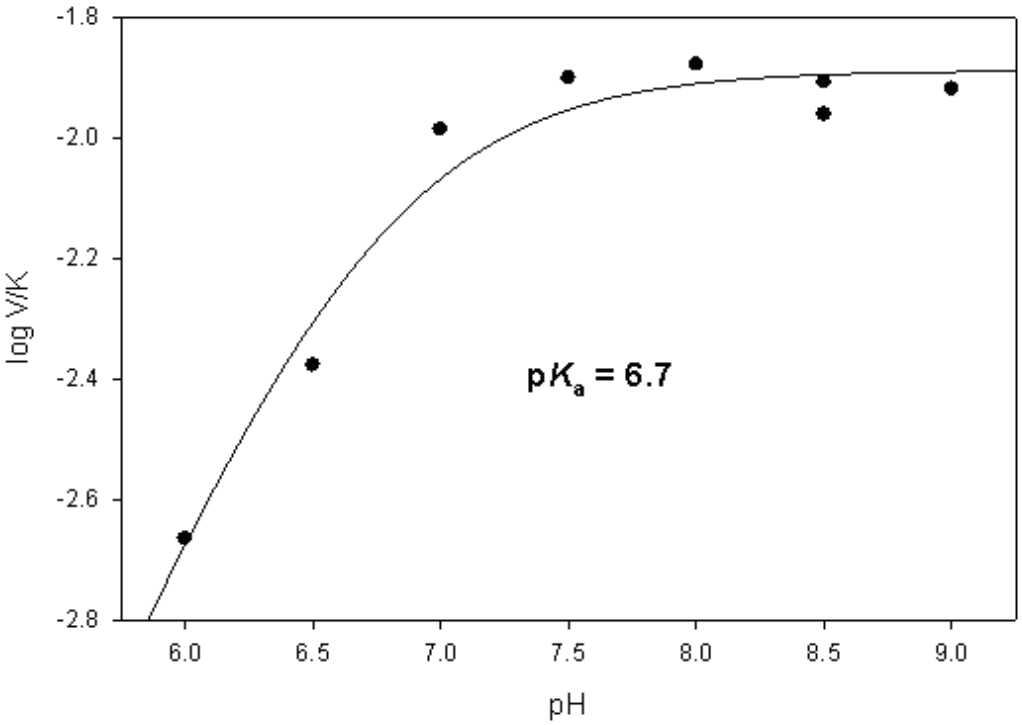

Figure 21 – KFA pH Dependence Plot (log V/K)

Inhibition of KFA by addition of EDTA

To determine the effect of the chelating agent EDTA on KFA reaction kinetics, assays were conducted in which the concentration of NFK was held constant at 100 μM while the concentration of added EDTA was increased from 0 to 400 μM. Slopes obtained from each reaction were converted to velocities. A table of these velocities with their corresponding EDTA concentrations is displayed in Table 1.

Table 1 – KFA EDTA Inhibition Assay Results

[NFK] (μM)	[EDTA] (μM)	Avg. Velocity (μmol/min*mg
100	0	22.57
100	25	24.43
100	50	23.04
100	100	21.26
100	150	22.51
100	200	24.08
100	400	24.88

Inhibition of KFA by addition of Kynurenine

To determine whether KFA can be inhibited by its reaction product kynurenine, assays were conducted in which the concentration of NFK was held constant at 100 μM while the concentration of kynurenine was increased from 0 to 400 μM. The formation of kynurenine was monitored at 365 nm. Slopes obtained from each reaction were converted to velocities and fit to the Michaelis-Menten equation. The resulting plot is shown below in Figure 22. Upon reviewing the assay results it was evident that the 100 μM inhibition data point was an outlier and dramatically affected the interpretation of the data.

Therefore, a second plot was generated with this data point removed, shifting the intersection point of the trend lines to the y axis. This plot is shown in Figure 23.

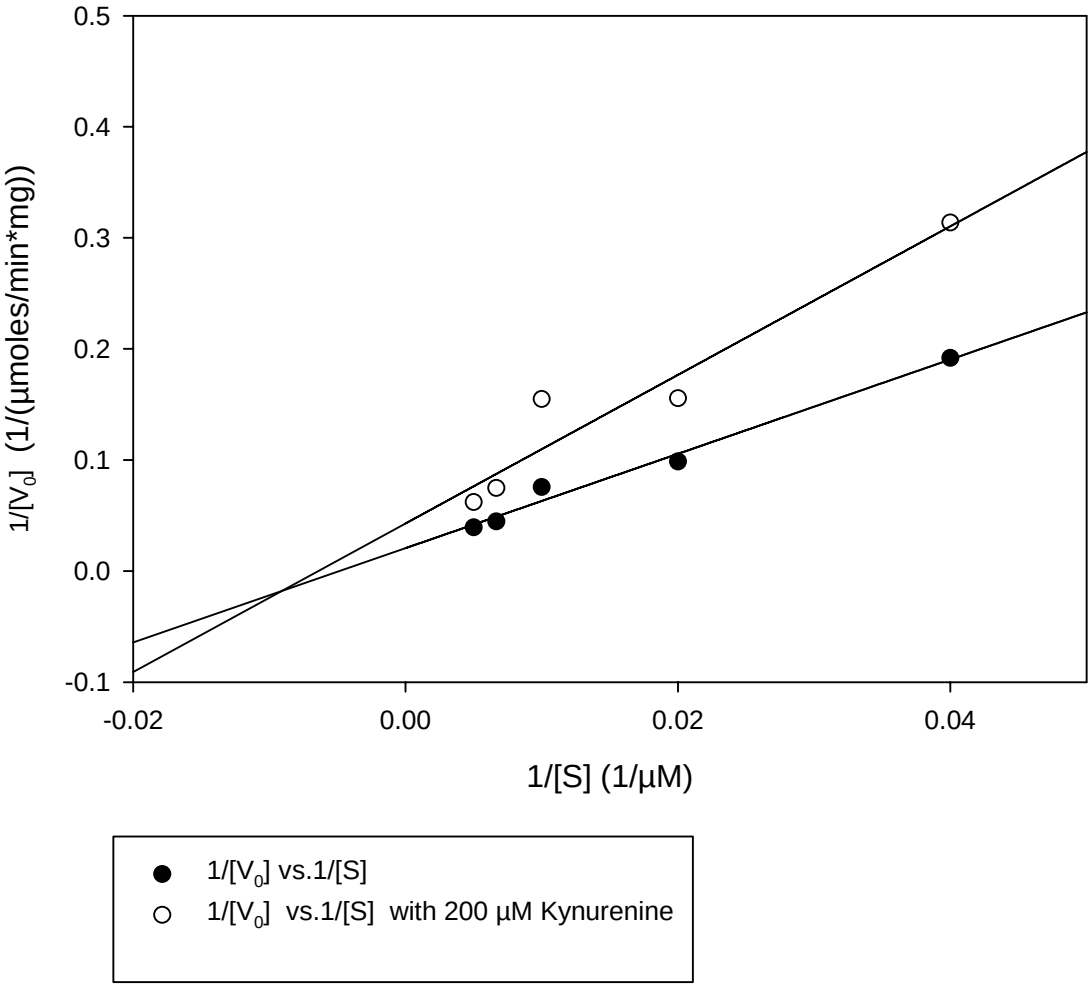

Figure 22 – KFA Product Inhibition Assay

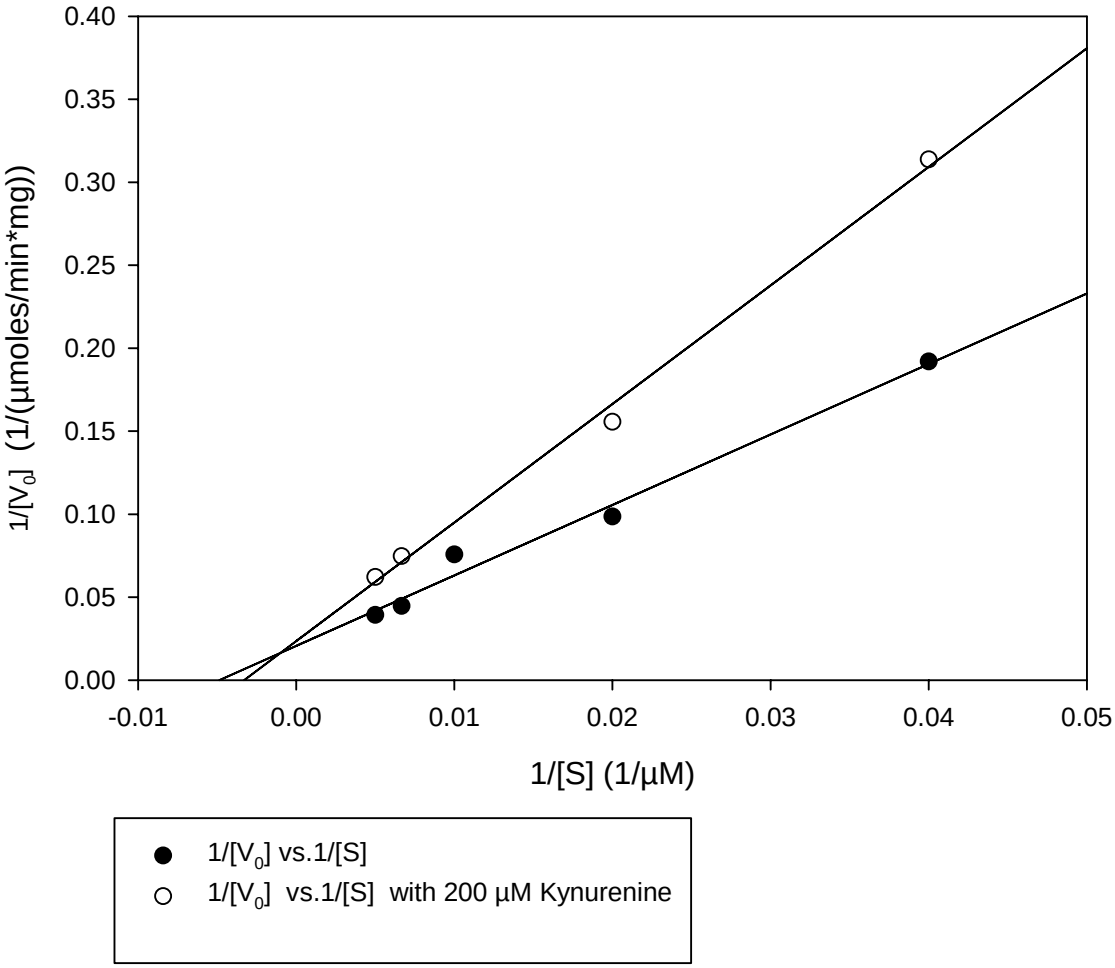

Figure 23 – KFA Product Inhibition Assay (with 200 µM data point removed)

Inhibition of KFA by addition of phenylmethylsulfonyl fluoride (PMSF)

To determine whether KFA can be inhibited by the serine protease inhibitor PMSF, inhibition assays were conducted using fixed concentrations of NFK while increasing the reaction concentration of PMSF. No inhibitory effect was observed on enzyme activity, mirroring the results obtained by Kurnasov and supporting the hypothesis that the active site structure of the enzyme is significantly different from that of the mammalian homolog. The results of this assay are shown in Figure 24 along with sodium bisulfite inhibition data (see following section). The V_{max} was determined to be 0.28 ± 0.02 μmol/min*mg and the K_m was determined to be 54 ± 8.5 μM.

Inhibition of KFA by addition of sodium bisulfite

To determine whether the KFA enzyme from *B. cereus* could be inhibited by sodium bisulfite in the same fashion that formamidase II from *S. parvulus* was inhibited [16, 30], activity assays were conducted which contained fixed concentrations of NFK and variable concentrations of sodium bisulfite. Marked inhibition was observed, with a 26% drop in activity occurring at a sodium bisulfite concentration of 10 mM, compared to the strong inhibition (30%) seen at 10 mM with *S. parvulus* formamidase II. The V_{max} for the inhibited reaction was determined to be 0.23 ± 0.03 μmol/min*mg and the K_m to be 51 ± 18 μM. The V_{max} for the uninhibited reaction was determined to be 0.31 ± 0.01 μmol/min*mg and the K_m to be 66 ± 5 μM.

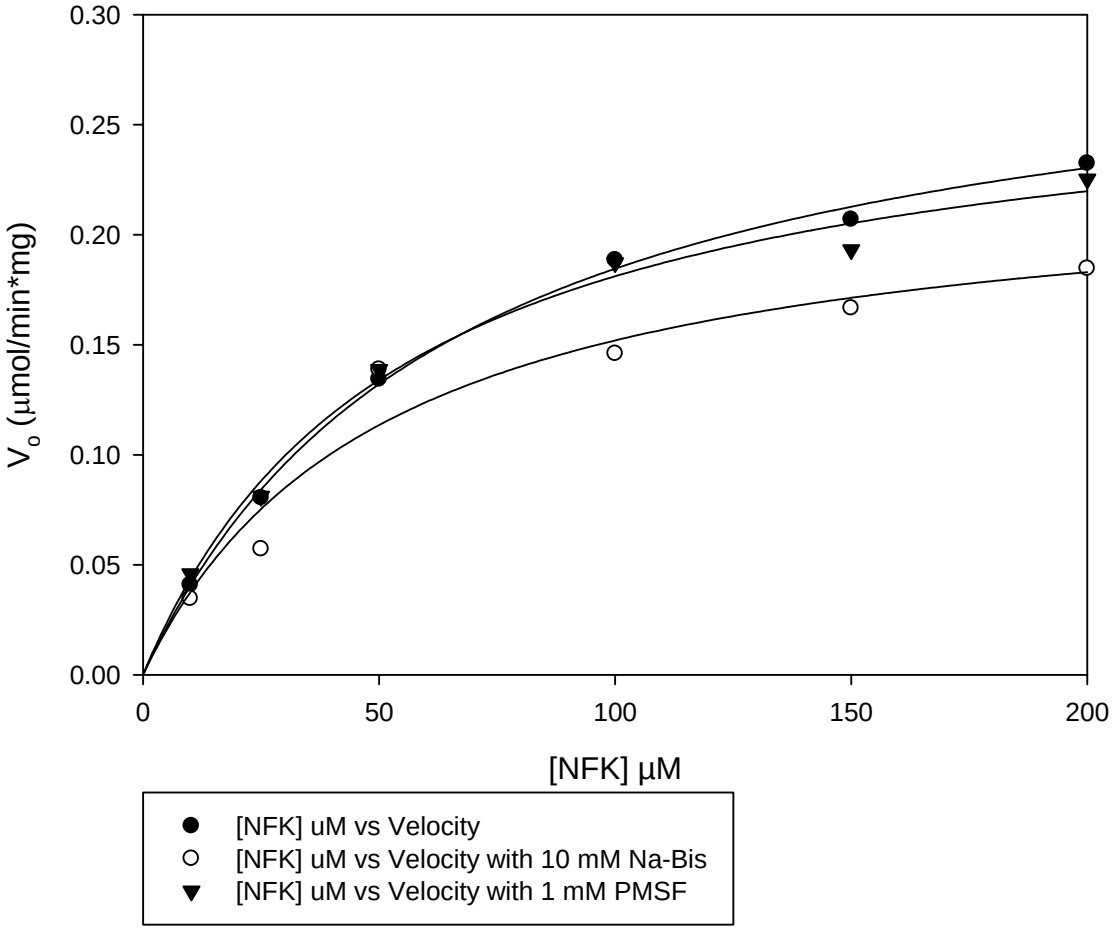

Figure 24 – Sodium Bisulfite and PMSF Inhibition Assays

VI. DISCUSSION

KFA Properties

KFA purified by Kurnasov *et al.* [24] was determined to have a molecular weight of 23.3 kDa as determined by SDS-PAGE. This result was consistent with the mass obtained in this study. By correlation with the mass published by Katz *et al*., we have likely purified the equivalent of formamidase II, the formamidase previously seen in *Streptomyces parvulus* to be active in the kynurenine pathway [30]. Ammonium sulfate was found to be extremely stabilizing, with a 10 mM solution causing the purified protein to slowly precipitate out of solution and form a fine white pellet. Activities observed immediately after purification were compared to those obtained from enzyme that had been stored for several months and were found to be nearly identical (data not shown).

KFA Kinetics

A table comparing the results of the saturation assays performed by Kurnasov *et al.* [14], [24], Katz *et al.* [16], and this study is shown in Table 3. Note that in some cases units used to represent the results in the literature were converted to those used in this study in order to facilitate comparisons.

Table 2 – Comparison of KFA Kinetic Data across Publications

Author	Bacterial Species	V_{max} (µmol/min*mg)	K_m (mM)	K_{cat} (1/s)	k_{cat}/K_m ($M^{-1}s^{-1}$)
Kurnasov [24]	*R. metallidurans*	ND**	0.075 ± 0.009	0.77 ± 0.03	1.03 X 10^4
Kurnasov [14]	*B. cereus*	~5.9	ND**	ND**	ND**
Katz [16]	*S. parvulus*	26.8	0.31	ND**	ND**
Bougie	*B. cereus*	68.5 ± 5	0.170 ± 0.020	31.1	1.82 X 10^5

**Not supplied by reference source

There is some variability between the values for each parameter in this table, although these differences are not so great as to call into question their overall agreement. Several factors could explain these differences. Perhaps the most obvious explanation is the fact that the enzymes assayed by each study, with the exception of Kurnasov's second study, were not from *B. cereus.* Additionally, both activity assays from Kurnasov and Begley were equilibrated at 37°C for 5 minutes prior to addition of enzyme, whereas the assays performed in this work were shaken upon addition of enzyme and conducted at room temperature. Katz *et al.* noted in that in their assays, formamidase II showed a significant decrease in activity above 30°C. Also of note is the fact that samples of KFA that do not contain a stabilizing agent lose activity fairly rapidly. All kinetic measurements assume 100% activity per aliquot of enzyme though this is patently false, regardless of efforts to prevent enzyme degradation. Without knowing the storage conditions used by the authors of the literature sources cited, it is impossible to know how their samples were kept. Finally, a general dearth of detailed experimental results

from the references cited provides some difficulty in comparing them to the results obtained in this work.

In addition to determining the basic kinetic parameters for the KFA reaction, pH assays were conducted in order to determine the optimum pH for KFA activity and to potentially shed light on the mechanism of the enzyme. The optimum pH for the reaction was approximately 8.0-8.5, and activity dropped precipitously below 6.0. The theoretical isoelectric point (pI) of KFA is 4.95 as determined using the ExPaSY ProtParam online program (http://www.expasy.ch/tools/protparam.html), which could explain the drop in activity seen at pH values less than 6 due by causing destabilization of the enzyme due to interrupted tertiary structure interactions. Since the enzyme's activity peaked in basic conditions, the rate limiting step of KFA catalysis possibly involves abstraction of a solvent proton by a basic functionality, or could depend on the generation of a nucleophilic functional group, such as with the formation of the alkoxide ion in the mechanism of chymotrypsin. Formation of such a nucleophilic species could be aided by increasing pH, resulting in lower energy catalytic group hydrogen bonding. In regard to KFA, this nucleophile could be a deprotonated water molecule, which could then attach to the *N*-formyl carbonyl carbon, resulting in the cleavage of formate and generation of L-kynurenine.

Four distinct inhibition assays were carried out to further elucidate the mechanism of KFA. The main product of the KFA reaction, kynurenine, was shown to exhibit competitive inhibition with NFK. This sheds light on the order of substrate binding and product release for KFA, as both molecules must bind to the same form of the enzyme in

order to compete with each other. In other words, a compulsory ordered bi-bi mechanism rather than a random or ping-pong mechanism is probably being used by the enzyme [31]. A proposed binding order is shown below:

Proposed Binding Order for KFA

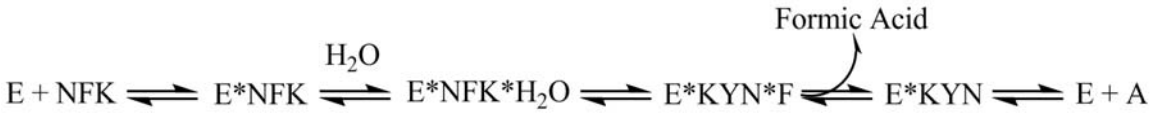

Next, KFA reactions in the presence of PMSF were conducted. PMSF is a known serine protease inhibitor which binds preferentially to active site serine residues. Addition of PMSF to the KFA reaction mixtures had no observable effect on the kinetics of the reaction, which confirms the findings of Kurnasov *et al.* [24] and supports the theory that the bacterial enzyme has a different active site and mechanism from the eukaryotic enzyme. Finally, inhibition studies using sodium bisulfite were conducted, as this compound, along with other ionic species, was shown to inhibit the formamidase II isolated from *Streptomyces parvulus [30]*. A 26% drop in V_{max} between the inhibited and uninhibited reactions was observed, compared to the 30% decrease in activity noted in the *S. parvulus* study. While the mechanism behind this inhibition is not clear, disulfide bonds could possibly be reduced by bisulfite. This would have the effect of disturbing the tertiary structure of the enzyme, thereby reducing activity. This result could imply that the formamidase we have isolated from *B. cereus* shares structural similarities with the formamidase II enzyme.

KFA has been documented in studies prior to this work as being a metal dependent hydrolase, in contrast to the eukaryotic enzyme which is a serine hydrolase [22]. This assumption was based on the results of enzymatic assays where EDTA was added as an inhibitor as well as the primary structure of the enzyme, which was found to have a metal binding motif indicative of a metal dependent hydrolase [14]. Interestingly, the same group that saw complete inhibition with EDTA observed no activation of the enzyme when additional zinc was added to the enzyme reaction mixture. Numerous reasons could account for this, such as an obscured metal binding pocket which requires adequate levels of zinc to be present before complete folding is achieved. Another possibility is that the enzyme is in fact not metal dependent. Attempts were made to activate the enzyme by addition of cobalt rather than zinc, again with no discernable effect. The results from the EDTA-KFA assays performed in this study contradict the inhibition seen by other groups [14, 24] but support the findings of Katz *et al.* [16].

KFA solvent kinetic isotope effects (SKIE) were determined in order to further investigate the potential presence of a catalytic metal ion. Normally, enzymatic reactions which make use of activated water as a nucleophile proceed faster in H_2O than in D_2O. This is due to the increased difficulty in abstracting a deuteron from oxygen than a proton, which is a result of the D-O bonds in a molecule of deuterium existing in a lower "energy well" than the H-O bonds of water [32]. A corollary to this principle exists when dealing with metal dependent enzymes, which generally display the opposite behavior expected in that the reactions they catalyze proceed faster in deuterium than in water if the rate-limiting step is metal-assisted deprotonation of water [32]. The SKIE data

obtained in this study graphically demonstrates that KFA has a normal isotope effect, which is indicative of either a non-metal dependent enzyme or a metal dependent enzyme whose rate-limiting step is not deprotonation of water.

VII. CONCLUSION

In this study we have obtained a basic kinetic profile for kynurenine formamidase from *B. cereus* and have provided results which directly contradict the findings of some of the work previously published by other groups concerning this enzyme, particularly regarding the metal dependency in the enzyme's mechanism. A lack of detailed results and methodology in these publications complicates interpretation of some of the data, as does the fact that the enzymes analyzed in these studies are from different bacterial species. Further studies on this aspect of the enzyme would be necessary to fully validate our findings. In particular, inductively coupled plasma atomic absorption spectroscopy would be a powerful technique which could be used to determine the presence or absence of metal in the enzyme and metal stoichiometries. Ultimately this work provides a solid foundation upon which further structural and mechanistic studies can build.

REFERENCES

REFERENCES

1. Deshpande, L.M., et al., *Antimicrobial resistance and molecular epidemiology of vancomycin-resistant enterococci from North America and Europe: a report from the SENTRY antimicrobial surveillance program.* Diagn Microbiol Infect Dis, 2007. **58**(2): p. 163-70.

2. Gordon, N.C. and D.W. Wareham, *Multidrug-resistant Acinetobacter baumannii: mechanisms of virulence and resistance.* Int J Antimicrob Agents. **35**(3): p. 219-26.

3. Kodmon, C., et al., *Multidrug- and extensively drug-resistant tuberculosis: a persistent problem in the European Union European Union and European Economic Area.* Euro Surveill. **15**(11).

4. Plata, K., A.E. Rosato, and G. Wegrzyn, *Staphylococcus aureus as an infectious agent: overview of biochemistry and molecular genetics of its pathogenicity.* Acta Biochim Pol, 2009. **56**(4): p. 597-612.

5. Palanichamy, K. and K.P. Kaliappan, *Discovery and syntheses of "superbug challengers"-platensimycin and platencin.* Chem Asian J. **5**(4): p. 668-703.

6. Griffin, M.O., et al., *Tetracyclines: a pleitropic family of compounds with promising therapeutic properties. Review of the literature.* Am J Physiol Cell Physiol, 2010. **299**(3): p. C539-48.

7. Foster, A.C., et al., *Kynurenic acid blocks neurotoxicity and seizures induced in rats by the related brain metabolite quinolinic acid.* Neurosci Lett, 1984. **48**(3): p. 273-8.

8. Jhamandas, K., et al., *Quinolinate-induced cortical cholinergic damage: modulation by tryptophan metabolites.* Brain Res, 1990. **529**(1-2): p. 185-91.

9. Stone, T.W. and L.G. Darlington, *Endogenous kynurenines as targets for drug discovery and development.* Nat Rev Drug Discov, 2002. **1**(8): p. 609-20.

10. Batabyal, D. and S.R. Yeh, *Human tryptophan dioxygenase: a comparison to indoleamine 2,3-dioxygenase.* J Am Chem Soc, 2007. **129**(50): p. 15690-701.

11. Belladonna, M.L., et al., *Immunosuppression via tryptophan catabolism: the role of kynurenine pathway enzymes.* Transplantation, 2007. **84**(1 Suppl): p. S17-20.

12. Guillemin, G.J., et al., *Characterization of the kynurenine pathway in human neurons.* J Neurosci, 2007. **27**(47): p. 12884-92.

13. Young, S.N. and M. Leyton, *The role of serotonin in human mood and social interaction. Insight from altered tryptophan levels.* Pharmacol Biochem Behav, 2002. **71**(4): p. 857-65.

14. Kurnasov, O., et al., *NAD biosynthesis: identification of the tryptophan to quinolinate pathway in bacteria.* Chem Biol, 2003. **10**(12): p. 1195-204.

15. Begley, T.P., et al., *The biosynthesis of nicotinamide adenine dinucleotides in bacteria.* Vitam Horm, 2001. **61**: p. 103-19.

16. Katz, E., D. Brown, and M.J. Hitchcock, *Arylformamidase from Streptomyces parvulus.* Methods in Enzymology, 1987. **142**: p. 225-34.

17. Dobrovolsky, V.N., et al., *Effect of arylformamidase (kynurenine formamidase) gene inactivation in mice on enzymatic activity, kynurenine pathway metabolites and phenotype.* Biochim Biophys Acta, 2005. **1724**(1-2): p. 163-72.

18. Pabarcus, M.K. and J.E. Casida, *Kynurenine formamidase: determination of primary structure and modeling-based prediction of tertiary structure and catalytic triad.* Biochim Biophys Acta, 2002. **1596**(2): p. 201-11.

19. Pabarcus, M.K. and J.E. Casida, *Cloning, expression, and catalytic triad of recombinant arylformamidase.* Protein Expr Purif, 2005. **44**(1): p. 39-44.

20. Menge, U., *[Formamidase--microheterogeneity, catalytic properties and inhibitors (author's transl)].* Hoppe Seylers Z Physiol Chem, 1979. **360**(2): p. 185-96.

21. Arndt, J.W., et al., *Crystal structure of an alpha/beta serine hydrolase (YDR428C) from Saccharomyces cerevisiae at 1.85 A resolution.* Proteins, 2005. **58**(3): p. 755-8.

22. Wogulis, M., et al., *Identification of formyl kynurenine formamidase and kynurenine aminotransferase from Saccharomyces cerevisiae using crystallographic, bioinformatic and biochemical evidence.* Biochemistry, 2008. **47**(6): p. 1608-21.

23. Nardini, M. and B.W. Dijkstra, *Alpha/beta hydrolase fold enzymes: the family keeps growing.* Curr Opin Struct Biol, 1999. **9**(6): p. 732-7.

24. Kurnasov, O., et al., *Aerobic tryptophan degradation pathway in bacteria: novel kynurenine formamidase.* FEMS Microbiol Lett, 2003. **227**(2): p. 219-27.

25. Farrow, J.M., 3rd and E.C. Pesci, *Two distinct pathways supply anthranilate as a precursor of the Pseudomonas quinolone signal.* J Bacteriol, 2007. **189**(9): p. 3425-33.

26. de Kievit, T.R. and B.H. Iglewski, *Bacterial quorum sensing in pathogenic relationships.* Infect Immun, 2000. **68**(9): p. 4839-49.

27. Ziegler, K., et al., *Substrate analysis of homoserine acyltransferase from Bacillus cereus.* Biochem Biophys Res Commun, 2007. **361**(2): p. 510-5.

28. Takikawa, O., et al., *Mechanism of interferon-gamma action. Characterization of indoleamine 2,3-dioxygenase in cultured human cells induced by interferon-gamma and evaluation of the enzyme-mediated tryptophan degradation in its anticellular activity.* J Biol Chem, 1988. **263**(4): p. 2041-8.

29. Dalgliesh, C.E., *The Synthesis of N'-Formyl-DL-kynurenine, N-Acetyl-DL-kynurenine and Related Compounds, and Observations on the Synthesis of Kynurenine.* J. Chem. Soc., 1952: p. 137-141.

30. Brown, D., M.J. Hitchcock, and E. Katz, *Purification and characterization of kynurenine formamidase activities from Streptomyces parvulus.* Can J Microbiol, 1986. **32**(6): p. 465-72.

31. Cleland, W., *The kinetics of enzyme-catalyzed reactions with two or more substrates or products: I. Nomenclature and rate equations.* Biochimica et Biophysica Acta, 1963. **67**: p. 104-137.

32. Scheiner, S., *Calculation of isotope effects from first principles.* Biochim Biophys Acta, 2000. **1458**(1): p. 28-42.

CURRICULUM VITAE

James Marcus Bougie was born in Fairfax, Virginia. He graduated from Westfield High School in Chantilly, VA in 2004. He then attended George Mason University in Fairfax, VA and completed his Bachelor of Science in Chemistry in 2007. At the time of writing he is a research associate at the National Institutes of Health Center for Translational Therapeutics. He is expected to receive his Master of Science in Chemistry from George Mason University in December 2011